

## What $\pi$ - $\pi$ scattering tells us about chiral perturbation theory

J. Stern and H. Sazdjian

*Division de Physique Théorique, Institut de Physique Nucléaire, F-91406 Orsay Cedex, France*

N. H. Fuchs

*Department of Physics, Purdue University, West Lafayette, Indiana 47907*

(Received 13 January 1993)

We describe a rearrangement of the standard expansion of the symmetry-breaking part of the QCD effective Lagrangian that includes into each order additional terms which in the standard chiral perturbation theory ( $\chi$ PT) are relegated to higher orders. The new expansion represents a systematic and unambiguous generalization of the standard  $\chi$ PT, and is more likely to converge rapidly. It provides a consistent framework for a measurement of the importance of additional “higher order” terms whose smallness is usually assumed but has never been checked. A method of measuring, among other quantities, the QCD parameters  $\hat{m}\langle\bar{q}q\rangle$  and the quark mass ratio  $m_s/\hat{m}$  is elaborated in detail. The method is illustrated using various sets of available data. Both of these parameters might be considerably smaller than their respective leading-order standard  $\chi$ PT values. The importance of new, more accurate, experimental information on low-energy  $\pi$ - $\pi$  scattering is stressed.

PACS number(s): 11.30.Rd, 11.40.Fy, 13.75.Lb

### I. INTRODUCTION

Owing to quark confinement, the connection between QCD correlation functions and hadronic observables is far from being straightforward. In the low-energy domain, such a connection is described by chiral perturbation theory ( $\chi$ PT) [1–3]. The latter provides a complete parametrization (in terms of an effective Lagrangian) of low-energy off-shell correlation functions of quark bilinears, which should take into account (i) the normal and anomalous Ward identities of chiral symmetry, explicitly broken by quark masses; (ii) spontaneous breakdown of chiral symmetry; and (iii) analyticity, unitarity, and crossing symmetry. On the other hand, such a parametrization (effective Lagrangian) should be sufficiently general, and should not introduce any additional dynamical assumptions beyond those listed above that could be hard to identify as emerging from QCD. The specificity of QCD then resides in numerical values of low-energy constants, which characterize the above parametrization. The theoretical challenge is to calculate these low-energy parameters from the fundamental QCD Lagrangian. While such a calculation is awaited, these parameters can be subjected to experimental investigation. Chiral symmetry guarantees that the same parameters that are introduced through the low-energy expansion of QCD correlation functions also define the low-energy expansion of hadronic observables—pseudoscalar meson masses, transition and scattering amplitudes.

In this paper, a new method will be elaborated that allows a detailed measurement of certain low-energy parameters, using the  $\pi$ - $\pi$  elastic scattering data [2,4]. Instead of concentrating on a particular set of scattering lengths and effective ranges [2] whose extraction from

experimental data is neither easy nor accurate, emphasis will be put on a detailed fit of the scattering amplitude in a whole low-energy domain of the Mandelstam plane, including the unphysical region. In this way it is possible to obtain some *experimental* insight on the low-energy parameter  $2\hat{m}B_0$ , where  $\hat{m}$  is the average of the up and down quark masses,  $B_0$  is the condensate

$$B_0 = -\frac{1}{F_0^2}\langle 0|\bar{u}u|0\rangle = -\frac{1}{F_0^2}\langle 0|\bar{d}d|0\rangle = -\frac{1}{F_0^2}\langle 0|\bar{s}s|0\rangle, \quad (1.1)$$

and  $|0\rangle$  and  $F_0$  stand for the ground state and pion decay constant, respectively, at  $m_u = m_d = m_s = 0$ . It is usually *assumed* that the parameter  $2\hat{m}B_0$  differs from the pion mass squared by not more than 1–2% [3], and the standard chiral perturbation theory could hardly tolerate an important violation of this assumption [5]. On the other hand, this assumption has never been confronted with experiment otherwise than indirectly—through the Gell-Mann–Okubo formula for pseudoscalar meson masses [5]. However, even the latter represents at best a consistency argument rather than a proof: The Gell-Mann–Okubo formula can hold quite independently of the relation between  $2\hat{m}B_0$  and  $M_\pi^2$  [6]. An independent measurement of  $2\hat{m}B_0$  is not only possible (as shown in the present work) but, for several reasons, it appears to be desirable.

(i) The effective Lagrangian  $\mathcal{L}_{\text{eff}}$  contains, in principle, an infinite number of low-energy constants, which are all related to (gauge-invariant) correlation functions of massless QCD. Among them,  $B_0$  plays a favored role: The order of magnitude of all low-energy constants other than  $B_0$  can be estimated using sum-rule techniques [7], which naturally bring in the scale  $\Lambda \sim 1$  GeV charac-

teristic of massive bound states. The expected order of magnitude of a low-energy constant related to a connected  $N$ -point ( $N > 1$ ) function of quark bilinears  $\bar{q}\Gamma q$ , which is not suppressed by the Zweig rule or by a symmetry, is  $F_0^2 \Lambda^{2-N}$  multiplied by a dimensionless constant of order 1. If quarks were not confined [8], a similar estimate would relate  $B_0$  and the mass of asymptotic fermion states with quark quantum numbers. However, in a confining theory, no similar relation between  $B_0$  and the spectrum of massive bound states can be derived:  $\bar{q}q$  is an irreducible color singlet and there is no complete set of intermediate states that could be inserted into the matrix element  $\langle 0|\bar{q}q|0\rangle$ .  $B_0$  could be as large as  $\Lambda \sim 1$  GeV or as small as the fundamental order parameter of chiral symmetry breaking,  $F_0 \sim 90$  MeV. *A priori*, there is no way to decide in favor of one of these scales, at least before the nonperturbative sector of QCD is controlled analytically or by reliable numerical methods, using, for instance, sufficiently large lattices. In this paper, we suggest how the question of the scale of  $B_0$  can be addressed experimentally.

(ii) To the extent that  $2\hat{m}B_0$  and  $(m_s + \hat{m})B_0$  are close to  $M_\pi^2$  and  $M_K^2$ , respectively, the ratio of quark masses

$$r \equiv m_s/\hat{m} \quad (1.2)$$

must approach  $2M_K^2/M_\pi^2 - 1 = 25.9$  [5,9]. There exists an independent measurement of the ratio  $r$  in terms of observed deviations from the Goldberger-Treiman relation [10] in nonstrange and strange baryon channels. This model-independent measurement indicates a considerably lower value for  $r$  than 25.9, unless the pion-nucleon coupling constant turns out to be below the value given by Koch and Pietarinen [11] by at least 4–5 standard deviations [12].

(iii) A reformulation of  $\chi$ PT, which allows  $2\hat{m}B_0$  to be considerably lower than  $M_\pi^2$ , has been given in Ref. [6]. It is as systematic and unambiguous as the standard  $\chi$ PT itself and is particularly suitable in the case where  $B_0$  is as small as  $F_\pi$ . It is based on a different expansion of the same effective Lagrangian, with the same infinity of independent terms. To all orders, the two perturbative schemes are identical, but, in each finite order, they can (but need not) substantially differ. For each given order, the new scheme contains more parameters than the standard  $\chi$ PT, the latter being reproduced for special values of these additional parameters. Already at the leading order  $O(p^2)$ , the new scheme contains one additional free parameter:

$$\eta = \frac{2\hat{m}B_0}{M_\pi^2}. \quad (1.3)$$

If  $\eta$  is set equal to 1, one recovers the leading  $O(p^2)$  order of the standard  $\chi$ PT. The new expansion can therefore be formally viewed as a *generalization* of the standard scheme and, in this sense, it will be referred to as *improved  $\chi$ PT*, since it aims to improve the convergence of the standard perturbation theory. Demonstrating that such an improvement is irrelevant, by measuring, for instance, the ratio (1.3) and finding it close to unity, would be an important experimental argument in favor of the

standard  $\chi$ PT.

(iv) In some cases, the convergence of standard  $\chi$ PT actually appears to be rather slow. Most of the indications in this direction can be traced back to the fact that the leading  $O(p^2)$  order of the standard  $\chi$ PT underestimates the Goldstone boson interaction and, in particular, the  $\pi$ - $\pi$  scattering amplitude. This manifests itself through virtual processes and/or final-state interactions, as in  $\gamma\gamma \rightarrow \pi^0\pi^0$  [13],  $\eta - 3\pi$  [14], etc. It might even be that although the next order  $O(p^4)$  improves the situation, it fails to reach the precision we may rightly expect from it. For example, the  $I = 0$   $s$ -wave  $\pi$ - $\pi$  scattering length, which is  $a_0^0 = 0.16$  in leading order [15], gets shifted to  $a_0^0 = 0.20$  by  $O(p^4)$  corrections [2], while the “experimental value” [16–18] is  $a_0^0 = 0.26 \pm 0.05$ . (In this paper it will be argued that scattering lengths are not the best quantities to look at. A more detailed amplitude analysis will reveal a possible amplification of the discrepancy, which exceeds one standard deviation.)

(v)  $\chi$ PT should be merely viewed as a theoretical framework for a precise measurement of low-energy QCD correlation functions. Its predictive power rapidly decreases with increasing order in the chiral expansion: More new parameters enter at each order and more experimental data have to be included to pin them down. For this reason, a slow convergence rate might sometimes lead to a qualitatively wrong conclusion with respect to a measurement based only on the first few orders. This might concern, in particular, the measurement of the ratio  $\eta$  (1.3) within the standard  $\chi$ PT. In the corresponding leading order,  $\eta$  is fixed to be 1, independently of any experimental data. This property of standard  $\chi$ PT could bias the measurement of  $\eta$  if  $\eta$  turned out to be considerably different from 1: One would presumably have to go to a rather high order and include a large set of data to discover the truth. In this case, the *improved  $\chi$ PT* would be a more suitable framework to measure  $\eta$  faithfully. The reason is that in the improved  $\chi$ PT,  $\eta$  is a *free parameter* from the start: It defines the *leading order  $\pi$ - $\pi$  amplitude*. Neglecting, for simplicity, Zweig-rule violation (cf. Ref. [6] and Sec. IV A), the latter reads

$$A(s|tu) = \frac{1}{F_0^2}(s - \eta M_\pi^2). \quad (1.4)$$

Using in this formula the value of  $a_0^0 = 0.26 \pm 0.05$ , one concludes that  $\eta = 0.4 \pm 0.4$  already at the leading order. The measurement then has more chances to saturate rapidly, say, at the one-loop level, provided  $\eta$  is much closer to  $0.4 \pm 0.4$  than to 1. The same remark applies to measurements of the quark mass ratio  $r = m_s/\hat{m}$ , which, incidentally, is closely related to  $\eta$  [10]: A slow convergence of the standard  $\chi$ PT could lower the leading-order result  $r = 25.9$  by considerably more than the usually quoted 10–20% [3,19].

(vi) The question of the actual value of  $\eta$  and/or of  $r = m_s/\hat{m}$  has to be settled experimentally. None of the known properties of QCD, nor the fact that light quark masses are tiny compared with the hadronic scale  $\Lambda \sim 1$  GeV, imply that  $\eta$  should be close to 1 and that  $r$  should be close to 25.9. The proof of this negative statement is provided by the existence of a mathematically consistent

generalization of the standard  $\chi$ PT that does not contradict any known fundamental property of QCD and allows for any value of  $\eta$  between 0 and 1 (and for any value of  $r$  between 6.3 and 25.9) [6]. Only in the special case of  $\eta$  and  $r$  close to 1 and 25.9, respectively, can the standard  $\chi$ PT claim a decent rate of convergence.

In Sec. II, the precise mathematical definition of the improved  $\chi$ PT, in terms of the effective Lagrangian, is briefly summarized. It is not a purpose of this paper to present a full formal development of this theory; incidentally, most of it can be read off from existing calculations [3] after rather minor extensions (which will be presented elsewhere). Here, we will mainly concentrate on phenomenological aspects of the problem in connection with low-energy  $\pi$ - $\pi$  scattering. The content of Sec. III is independent of any particular  $\chi$ PT scheme. In that section, a new low-energy representation of the  $\pi$ - $\pi$  scattering amplitude is given that provides the most general solution of analyticity, crossing symmetry, and unitarity up to and including the chiral order  $O(p^6)$ . (Partial wave projections of this representation coincide with a particular truncation of the well-known Roy equations [20].) Subsequently, this representation is used both to constrain the experimental data and to perform a comparison with theoretical amplitudes as predicted by the two versions of  $\chi$ PT. For the case of the improved  $\chi$ PT, the one-loop amplitude is worked out in Sec. IV. Finally, a method permitting a detailed fit of the experimental amplitude in a whole low-energy domain of the Mandelstam plane is developed in Sec. V. This method is then applied to various sets of existing data.

## II. FORMULATION OF IMPROVED $\chi$ PT

Following rather closely the off-shell formalism that was elaborated some time ago by Gasser and Leutwyler [3], we consider the generating functional  $Z(v^\mu, a^\mu, \chi)$  of connected Green's functions made up from  $SU(3) \times SU(3)$  vector and axial-vector currents as well as from scalar and pseudoscalar quark densities, as defined in QCD with three massless flavors. The sources  $v^\mu$ ,  $a^\mu$ , and  $\chi$  are specified through the Lagrangian

$$\mathcal{L} = \mathcal{L}_{\text{QCD}} + \bar{q}(\not{\psi} + \not{\phi}\gamma_5)q - \bar{q}_R\chi q_L - \bar{q}_L\chi^\dagger q_R, \quad (2.1)$$

which defines the vacuum-to-vacuum amplitude  $\exp(iZ)$ . Here,  $q_{L,R} = \frac{1}{2}(1 \mp \gamma_5)q$  stand for the light quark fields  $u$ ,  $d$ ,  $s$ , and  $\mathcal{L}_{\text{QCD}}$  is invariant under global  $SU(3) \times SU(3)$  transformations of  $q_L$  and  $q_R$ .  $v^\mu$  and  $a^\mu$  are traceless and Hermitian, whereas

$$\chi = s + ip \quad (2.2)$$

is a general  $3 \times 3$  complex matrix ( $s$  and  $p$  are Hermitian). Explicit chiral symmetry breaking by quark masses is accounted for by expanding  $Z$  around the point

$$v^\mu = a^\mu = 0, \quad \chi = \mathcal{M}_q \equiv \begin{pmatrix} m_u & & \\ & m_d & \\ & & m_s \end{pmatrix}. \quad (2.3)$$

The scalar-pseudoscalar source  $\chi$  and the quark mass matrix  $\mathcal{M}_q$  are closely tied together by chiral symmetry. (Notice that our source  $\chi$  differs from the  $\chi$  defined in Ref. [3] by a factor of  $2B_0$ .)

Instead of calculating  $Z$ , the effective theory parametrizes it by means of an effective Lagrangian, which depends on the sources and on eight Goldstone boson fields

$$U(x) = \exp\left(\frac{i}{F_0} \sum_{a=1}^8 \lambda^a \varphi_a(x)\right). \quad (2.4)$$

Leaving aside anomaly contributions described by the Wess-Zumino action, the effective Lagrangian  $\mathcal{L}_{\text{eff}}(U, v^\mu, a^\mu, \chi)$  is merely restricted by the usual space-time symmetries and by the requirement of invariance under local chiral transformations  $[\Omega_{L,R} \in SU(3)]$ ,

$$U(x) \rightarrow \Omega_R(x)U(x)\Omega_L^\dagger(x), \quad \chi(x) \rightarrow \Omega_R(x)\chi(x)\Omega_L^\dagger(x), \quad (2.5)$$

compensated by the inhomogeneous transformation of the sources  $v^\mu$  and  $a^\mu$ :

$$v^\mu + a^\mu \rightarrow \Omega_R(v^\mu + a^\mu + i\partial^\mu)\Omega_R^\dagger, \quad (2.6)$$

$$v^\mu - a^\mu \rightarrow \Omega_L(v^\mu - a^\mu + i\partial^\mu)\Omega_L^\dagger.$$

(This gauge invariance of the nonanomalous part of  $Z$  is necessary and sufficient to reproduce all  $SU(3) \times SU(3)$  Ward identities.) Otherwise, the effective Lagrangian remains unrestricted.

$\mathcal{L}_{\text{eff}}$  can be written as an infinite series of local terms:

$$\mathcal{L}_{\text{eff}} = \sum_{n,m} \ell^{nm} \mathcal{L}_{nm}, \quad (2.7)$$

where  $\mathcal{L}_{nm}$  denotes an invariant under the transformations (2.5) and (2.6) that contains the  $n$ th power of the covariant derivatives  $D_\mu$  and the  $m$ th power of the scalar-pseudoscalar source  $\chi$ . The sum over independent invariants that belong to the same pair of indices  $(n, m)$  is understood. The covariant derivatives are defined as

$$D_\mu U = \partial_\mu U - i(v_\mu + a_\mu)U + iU(v_\mu - a_\mu), \quad (2.8)$$

and likewise for  $D_\mu \chi$ . The expansion coefficients  $\ell^{nm}$  represent properly subtracted linear combinations of massless QCD correlation functions that involve  $n$  vector and/or axial-vector currents and  $m$  scalar and/or pseudoscalar densities, all taken at vanishing external momenta. The first two terms in the sum (2.7), for instance, read ( $n$  is even)

$$\ell^{01} \mathcal{L}_{01} = \frac{1}{2} F_0^2 B_0 \langle U^\dagger \chi + \chi^\dagger U \rangle, \quad (2.9)$$

$$\ell^{20} \mathcal{L}_{20} = \frac{1}{4} F_0^2 \langle D^\mu U^\dagger D_\mu U \rangle.$$

Everything said so far is rather general and independent of any particular perturbative scheme.

Chiral perturbation theory is an attempt to reorder the infinite sum (2.7) as

$$\mathcal{L}_{\text{eff}} = \sum_d \mathcal{L}^{(d)}, \quad (2.10)$$

where  $\mathcal{L}^{(d)}$  collects all terms that in the limit

$$p \rightarrow 0, \quad M_\pi \rightarrow 0, \quad p^2/M_\pi^2 \text{ fixed} \quad (2.11)$$

behave as  $O(p^d)$  ( $p$  stands for external momenta). In order to relate the expansions (2.10) and (2.7), one needs to know the *effective infrared dimension*  $d(m_q)$  of the quark mass. The invariant  $\mathcal{L}_{nm}$  then contributes as  $O(p^{d_{nm}})$ , where

$$d_{nm} = n + m d(m_q). \quad (2.12)$$

For infinitesimally small quark masses, one should have

$$d(m_q) = 2, \quad m_q \rightarrow 0. \quad (2.13)$$

This follows from the mathematical fact that, in QCD,

$$\lim_{m_q \rightarrow 0} \frac{(m_i + m_j)B_0}{M_P^2} = 1. \quad (2.14)$$

(Here,  $i, j = u, d, s$  and  $M_P$  is the mass of the pseudoscalar meson  $\bar{v}j$ ,  $i \neq j$ .) The assumption that in the *real world*, i.e., for physical values of quark masses, the effective dimension of the quark mass is 2, underlies the *standard*  $\chi$ PT. It amounts to the well-known rule that asserts that each insertion of the quark mass matrix and/or of the scalar-pseudoscalar source  $\chi$  counts as two powers of external momenta. Equivalently, the standard  $\chi$ PT can be viewed as an expansion around the limit

$$(p, m_q) \rightarrow 0, \quad p^2/M_P^2 \text{ fixed}. \quad (2.15)$$

Since, by definition, the low-energy constants  $\ell^{nm}$  are independent of quark masses, they are of order 1 in the limit (2.15).

It is easy to see that the convergence of the standard  $\chi$ PT could be seriously disturbed if  $B_0 \ll \Lambda \sim 1$  GeV, say if  $B_0 \sim 100$  MeV [6,10]. The expansion of  $M_P^2$  reads ( $i, j = u, d, s$ ;  $i \neq j$ )

$$M_P^2 = (m_i + m_j)B_0 + (m_i + m_j)^2 A_0 + \dots, \quad (2.16)$$

where the dots stand for nonanalytic terms and for higher-order terms.  $A_0$  can be expressed in terms of two-point functions of scalar and pseudoscalar quark densities divided by  $F_0^2$  [10]. It satisfies a superconvergent dispersion relation, whose saturation leads to the order of magnitude estimate  $A_0 \sim 1 - 5$ . For  $B_0$  as small as 100 MeV, the first- and second-order terms in Eq. (2.16) then become comparable for quark masses as small as (10–50) MeV. In order to accommodate this possibility, the *improved*  $\chi$ PT attributes to the quark mass *and* to the vacuum condensate parameter  $B_0$  the effective dimension 1,

$$d(m_q) = d(B_0) = 1, \quad (2.17)$$

reflecting their smallness compared to the scale  $\Lambda$ . This does not contradict mathematical statements such as (2.14). It only means that, although for physical values of quark masses the ratio in Eq. (2.14) remains on the order of 1, it is allowed to differ from 1 considerably.

To summarize, in the improved  $\chi$ PT each insertion of the quark mass matrix  $\mathcal{M}_q$  and/or of the scalar-pseudoscalar source  $\chi$  counts as a single power of external momentum (pion mass) *and so does the parameter*  $B_0$ . This leads to a new expansion of the effective Lagrangian

$$\mathcal{L}_{\text{eff}} = \sum_d \tilde{\mathcal{L}}^d, \quad (2.18)$$

where each  $\tilde{\mathcal{L}}^d$  contains more terms  $\mathcal{L}_{nm}$  than does the corresponding term  $\mathcal{L}^d$  in the case of the standard counting. The improved  $\chi$ PT is a simultaneous expansion in  $p/\Lambda$ ,  $m_q/\Lambda$ , and  $B_0/\Lambda$  around the limit

$$(p, m_q, B_0) \rightarrow 0, \quad p^2/M_P^2, \quad \text{and } m_q B_0/M_P^2 \text{ fixed}. \quad (2.19)$$

This is just another way to realize the chiral limit (2.11). The fact that, in the effective theory, we treat  $B_0$  as an arbitrary expansion parameter does not contradict the general belief that, within QCD, this parameter is fixed and, hopefully, calculable. After all, quantum electrodynamics is also based on an expansion in  $\alpha$ , in spite of the general belief that there might exist a more fundamental theory in which the value of  $\alpha$  is fixed and calculable [21].

### III. RECONSTRUCTION OF THE LOW-ENERGY $\pi$ - $\pi$ SCATTERING AMPLITUDE NEGLECTING $O(p^8)$ EFFECTS

The analysis of low-energy  $\pi$ - $\pi$  scattering, traditionally based on analyticity, crossing symmetry, and unitarity [22,16,20], considerably simplifies if, in addition, one takes into account the Goldstone character of the pion. First, in the chiral limit (2.11), higher ( $\ell \geq 2$ ) partial waves are suppressed. The reason stems from the fact that in the limit (2.11) the whole amplitude behaves as  $O(p^2)$ , and, furthermore, it does not contain light dipion bound-state poles. Unitarity then implies that the scattering amplitude is dominantly real, since its imaginary part behaves as  $O(p^4)$ . Analyticity then forces the leading  $O(p^2)$  part of the amplitude  $A(s|tu)$  to be a polynomial in the Mandelstam variables. Furthermore, higher-than-first-order polynomials are excluded: They would be  $O(p^2)$  only provided their coefficients blew up as  $M_\pi^2 \rightarrow 0$ , which would contradict the finiteness of the  $S$  matrix in the limit  $m_q \rightarrow 0$  with the external momenta kept fixed at a nonexceptional value. Finally, crossing symmetry allows one to express the  $O(p^2)$  part of the scattering amplitude  $A(s|tu)$  as

$$A_{\text{lead}}(s|tu) = \frac{\alpha}{3F_\pi^2} M_\pi^2 + \frac{\beta}{3F_\pi^2} (3s - 4M_\pi^2), \quad (3.1)$$

where  $\alpha, \beta$  are two dimensionless constants that are of order 1 in the chiral limit. The linear amplitude (3.1) does

not contribute to  $\ell \geq 2$  partial waves. Consequently, the latter behave in the chiral limit as  $O(p^4)$  and, owing to unitarity, the absorptive parts of  $\ell \geq 2$  waves are suppressed at least to  $O(p^8)$ . This conclusion holds independently of more quantitative predictions of  $\chi$ PT, which in the actual case merely concern the values of the two parameters  $\alpha$  and  $\beta$  in Eq. (3.1).

The second simplification resides in the suppression of inelasticities arising from intermediate states that consist of more than two Goldstone bosons. The behavior of  $n$ -pion invariant phase space in the chiral limit (2.11) is given by its dimension: It scales like  $p^{2n-4}$ . Amplitudes with an arbitrary number of external pion legs are dominantly  $O(p^2)$ . Consequently, the contribution of multipion ( $n > 2$ ) intermediate states to the absorptive part of the elastic  $\pi$ - $\pi$  amplitude is suppressed in the chiral limit at least to  $O(p^8)$ .

The smallness of higher partial waves and of inelasticities are of course well-known phenomenological facts [16]. It is important that these “remarkable accidents” (see p. 53 of [16]) can be put under the rigorous control of chiral power counting: The previous discussion suggests that a rather simple amplitude analysis of low-energy  $\pi$ - $\pi$  scattering can be performed *up to and including*  $O(p^6)$  contributions. In the following we confirm and elaborate this expectation in detail. It will be shown in particular that, neglecting  $O(p^8)$  contributions, the whole scattering amplitude can be expressed in terms of low-energy  $s$  and  $p$  wave phase shifts and six (subtraction) constants. (The latter are related to the experimental phase shifts *via* unitarity.) The resulting expression (3.2) will prove particularly useful both for constraining low-energy experimental data and for providing a basis for a confrontation of chiral perturbation theory up to two loops with experiment.

### A. Statement of the theorem

Let  $\Lambda$  denote a scale (slightly) below the threshold for production of non-Goldstone particles. The  $\pi$ - $\pi$  amplitude can be written as

$$\begin{aligned} \frac{3}{32\pi} A(s|tu) &= T(s) + T(t) + T(u) \\ &+ \frac{1}{3} [2U(s) - U(t) - U(u)] \\ &+ \frac{1}{3} [(s-t)V(u) + (s-u)V(t)] \\ &+ R_\Lambda(s|t, u). \end{aligned} \quad (3.2)$$

The remainder,  $R_\Lambda$ , behaves in the chiral limit as  $O(p^8)$  relative to the scale  $\Lambda$ : Up to possible logarithmic terms,

$$R_\Lambda = O([p/\Lambda]^8), \quad (3.3)$$

where  $p$  stands for external pion momenta. In practice,  $\Lambda \lesssim 1$  GeV. The functions  $T$ ,  $U$ , and  $V$  are analytic for  $s < 4M_\pi^2$ , whereas for  $4M_\pi^2 < s < \Lambda^2$  their discontinuities

are given by the three lowest partial wave amplitudes  $f_\ell^I(s)$ :<sup>1</sup>

$$\begin{aligned} \text{Im } T(s) &= \frac{1}{3} \{ \text{Im } f_0^0(s) + 2 \text{Im } f_0^2(s) \}, \\ \text{Im } U(s) &= \frac{1}{2} \{ 2 \text{Im } f_0^0(s) - 5 \text{Im } f_0^2(s) \}, \\ \text{Im } V(s) &= \frac{27}{2} \frac{1}{s - 4M_\pi^2} \text{Im } f_1^1(s). \end{aligned} \quad (3.4)$$

The real parts of the functions  $T$ ,  $U$ , and  $V$  are defined only up to polynomials

$$\begin{aligned} \delta T(s) &= x(s - \frac{4}{3}M_\pi^2), \\ \delta U(s) &= y_0 + y_1 s + y_2 s^2 + y_3 s^3, \\ \delta V(s) &= -(y_1 + 4M_\pi^2 y_2 + 16M_\pi^4 y_3) \\ &\quad + (y_2 + 12M_\pi^2 y_3)s - 3y_3 s^2, \end{aligned} \quad (3.5)$$

where  $x$  and the  $y$ 's are five arbitrary real constants: Because of the relation  $s + t + u = 4M_\pi^2$ , the two sets of amplitudes  $T, U, V$  and  $T + \delta T, U + \delta U, V + \delta V$  lead to the same scattering amplitude  $A$ . [It is shown in Appendix B that Eqs. (3.5) actually represent the most general transformation of  $T, U, V$  leaving the scattering amplitude invariant.] After conveniently fixing the “gauge freedom” (3.5), the functions  $T$ ,  $U$ , and  $V$  can be written as

$$\begin{aligned} T(s) &= t_0 + t_2 s^2 + t_3 s^3 + \frac{s^3}{\pi} \int_{4M_\pi^2}^{\Lambda^2} \frac{dx}{x^3} \frac{1}{x-s} \text{Im } T(x), \\ U(s) &= \frac{s^3}{\pi} \int_{4M_\pi^2}^{\Lambda^2} \frac{dx}{x^3} \frac{1}{x-s} \text{Im } U(x), \\ V(s) &= v_1 + v_2 s + v_3 s^2 + \frac{s^2}{\pi} \int_{4M_\pi^2}^{\Lambda^2} \frac{dx}{x^2} \frac{1}{x-s} \text{Im } V(x), \end{aligned} \quad (3.6)$$

where the imaginary parts are given by Eqs. (3.4) and the  $t$ 's and  $v$ 's are constants. It will be shown shortly that Eq. (3.2) is a rigorous consequence of analyticity and crossing symmetry and of the Goldstone nature of the pion.

### B. Unitarity

The low-energy representation (3.2) of the scattering amplitude is exact up to an  $O(p^8)$  remainder. In the whole interval  $4M_\pi^2 < s < \Lambda^2$ , unitarity can be imposed with the same accuracy in terms of partial waves  $f_\ell^I$ . As already pointed out, deviations from the unitarity condition

$$\text{Im } f_\ell^I(s) = \sqrt{\frac{s - 4M_\pi^2}{s}} |f_\ell^I(s)|^2$$

above the inelastic threshold are of the order  $O(p^8)$ . The

<sup>1</sup>Notation and normalization are reviewed in Appendix A.

amplitude (3.2) contains all partial waves. For  $\ell \geq 2$ , the partial waves are real. Nevertheless, unitarity automatically is satisfied for  $\ell \geq 2$  up to  $O(p^8)$  terms, since higher partial waves anyway are  $O(p^4)$  or smaller. Consequently, it is sufficient to impose unitarity for the three lowest waves  $f_0^0$ ,  $f_1^1$ , and  $f_2^0$  (hereafter denoted as  $f_a$ ,  $a = 0, 1, 2$  according to their isospin). Projections of Eq. (3.2) into the three lowest partial waves read

$$\begin{aligned} \text{Re } f_a(s) &= P_a(s) + \frac{s^3}{\pi} \int_{4M_\pi^2}^{\Lambda^2} \frac{dx \text{Im } f_a(x)}{x^3 (x-s)} \\ &+ \frac{1}{\pi} \int_{4M_\pi^2}^{\Lambda^2} \frac{dx}{x} \sum_{b=0}^2 W_{ab}(s, x) \text{Im } f_b(x) + O(p^8) \end{aligned} \quad (3.7a)$$

for the two  $s$  waves ( $a = 0, 2$ ), whereas the  $p$  wave projection is

$$\begin{aligned} \text{Re } f_1(s) &= P_1(s) + \frac{s^2(s - 4M_\pi^2)}{\pi} \\ &\times \int_{4M_\pi^2}^{\Lambda^2} \frac{dx}{x^2(x - 4M_\pi^2)} \frac{\text{Im } f_1(x)}{x-s} \\ &+ \frac{1}{\pi} \int_{4M_\pi^2}^{\Lambda^2} \frac{dx}{x} \sum_{b=0}^2 W_{1b}(s, x) \text{Im } f_b(x) + O(p^8). \end{aligned} \quad (3.7b)$$

Here,  $P_a(s)$  are third-order polynomials whose coefficients are defined in terms of the six constants  $t_0, t_2, t_3$  and  $v_1, v_2, v_3$  which appear in Eqs. (3.6). These polynomials are tabulated in Appendix C, together with the nine kernels  $W_{ab}(s, x)$ , which define the left-hand cut contributions to the partial waves.

Equations (3.7a) and (3.7b) may be viewed as a particular truncation of the infinite system of Roy equations, which slightly differs from the form in which these equations have been used in the past [23]. Here, the truncation in angular momentum and energy is performed under the systematic control of chiral power counting. In particular, Eqs. (3.7a) and (3.7b) do not require a model-dependent evaluation of “driving terms,” which in the standard treatment behave in the chiral limit as  $O(p^4)$ , owing to the use of twice-subtracted dispersion relations. The price to pay is the occurrence of six (*a priori* unknown) constants in the polynomials  $P_a(s)$  instead of only two constants (usually, the two  $s$  wave scattering lengths), which characterize the inhomogeneous terms in standard Roy equations [20,23].

Equations (3.7a) and (3.7b) can be used to fully reconstruct from the data the *whole amplitude*  $A(s|tu)$  up to and including accuracy  $O(p^6)$  in the whole low-energy domain of the Mandelstam plane, including the unphysical region. For this purpose one has to know the absorptive parts of three lowest partial waves for  $4M_\pi^2 < s < \Lambda^2$  and the six constants  $t_0, t_2, t_3, v_1, v_2, v_3$ . Suppose one knew  $\text{Im } f_a(s)$  with associated error bars in the whole interval  $4M_\pi^2 < s < \Lambda^2 \lesssim 1 \text{ GeV}^2$ . Then one could calculate the dispersion integrals on the right-hand side of Eqs. (3.7a) and (3.7b). One would then determine the constants  $t$

and  $v$  from the best fit to the values  $\text{Re } f_a(s)$  determined from the input  $\text{Im } f_a(s)$  via the unitarity condition. The  $\chi^2$  of this fit may be considered as a measure of the internal consistency of the input data  $\text{Im } f_a(s)$ . In practice, *experimental* information on  $\text{Im } f_a(s)$  is only available for  $s$  well above the threshold. In this case, a more sophisticated iteration procedure [24] of Eqs. (3.7a) and (3.7b) has to be used in order (i) to extrapolate the experimental data down to the threshold and, simultaneously, (ii) to determine the six constants  $t$  and  $v$ . In both cases, the resulting amplitude is given by the formula (3.2).

### C. Proof of the reconstruction theorem

Formulas (3.2) and (3.6) can be proven following the original derivation of the Roy equations [20]. The proof is based on fixed- $t$  dispersion relations for the three  $s$ -channel isospin amplitudes  $F^{(I)}$ ,

$$\mathbf{F}(s, t, u) = \begin{pmatrix} F^{(0)} \\ F^{(1)} \\ F^{(2)} \end{pmatrix} (s, t, u), \quad (3.8)$$

combined with the crossing symmetry relations

$$\mathbf{F}(s, t, u) = C_{su} \mathbf{F}(u, t, s) = C_{st} \mathbf{F}(t, s, u) = C_{ut} \mathbf{F}(s, u, t). \quad (3.9)$$

(Properties of the crossing matrices  $C_{su}$ ,  $C_{st}$ , and  $C_{ut}$  are reviewed in Appendix A.) The standard Roy equations are derived from twice-subtracted dispersion relations—cf. the minimal number of subtractions required by the Froissart bound. In this case, however, the high-energy tail of the dispersion integral, which is hard to control in a model independent way, contributes to the  $O(p^4)$  part of the amplitude. (In standard Roy equations, this contribution is contained in the so-called driving terms [23].) If, on the other hand, one requires at low energy the precision  $O(p^4)$  or higher, then it is more appropriate to stick to less predictive *triply subtracted* fixed- $t$  dispersion relations:

$$\begin{aligned} \mathbf{F}(s, t) &= C_{st} \{ \mathbf{a}_+(t) + (s-u) \mathbf{b}_-(t) + (s-u)^2 \mathbf{c}_+(t) \} \\ &+ \frac{1}{\pi} \int_{4M_\pi^2}^{\infty} \frac{dx}{x^3} \left\{ \frac{s^3}{x-s} + \frac{u^3}{x-u} C_{su} \right\} \text{Im } \mathbf{F}(x, t). \end{aligned} \quad (3.10)$$

Here the subscript  $\pm$  refers to the eigenvalues  $\pm 1$  of the crossing matrix  $C_{tu}$ . [Notice that in the  $s$ -channel isospin basis (3.8),  $C_{tu} = \text{diag}(+1, -1, +1)$ .] The subtraction term then represents the most general quadratic function in  $s$  (for fixed  $t$ ) symmetric under  $s$ - $u$  crossing. By construction, the dispersion integral in Eq. (3.10) exhibits  $s$ - $u$  crossing symmetry too. The task is now to impose the remaining two crossing relations and to determine the subtraction functions  $\mathbf{a}$ ,  $\mathbf{b}$ , and  $\mathbf{c}$ . This can be achieved, neglecting in Eq. (3.10) contributions of chiral order  $O(p^8)$  and higher.

Let  $\Lambda$  be a scale set by the threshold of production of non-Goldstone particles. Let us split the dispersion integral in Eq. (3.10) into low-energy ( $x \leq \Lambda^2$ ) and high-energy ( $x > \Lambda^2$ ) parts. For  $4M_\pi^2 < s < \Lambda^2$ , the imaginary part can be written as

$$\begin{aligned} \text{Im } \mathbf{F} = & \text{Im } \Phi_+(s) + \left(1 + \frac{2t}{s - 4M_\pi^2}\right) \text{Im } \Phi_-(s) \\ & + \mathbf{A}_{\ell \geq 2}(s, t), \end{aligned} \quad (3.11)$$

where the first two terms stand for the contributions of  $s$  and  $p$  waves:

$$\text{Im } \Phi_+(s) = \begin{pmatrix} \text{Im } f_0^0(s) \\ 0 \\ \text{Im } f_0^2(s) \end{pmatrix}, \quad (3.12)$$

$$\text{Im } \Phi_-(s) = \begin{pmatrix} 0 \\ 3 \text{Im } f_1^1(s) \\ 0 \end{pmatrix}.$$

$\mathbf{A}_{\ell \geq 2}$  then collects the absorptive parts of all higher partial waves. The reason for this particular splitting resides in the chiral counting mentioned at the beginning of this section: The first two terms in Eq. (3.11) dominantly behave as  $O(p^4)$ , whereas  $\mathbf{A}_{\ell \geq 2}$  is suppressed to  $O(p^8)$ . The dispersion integral  $\mathbf{I}(s, t)$  in Eq. (3.10) then splits into three parts:

$$\mathbf{I}(s, t) = \mathbf{I}_{\ell < 2}(s, t) + \mathbf{I}_{\ell \geq 2}(s, t) + \mathbf{I}_H(s, t). \quad (3.13)$$

$\mathbf{I}_{\ell < 2}$  ( $\mathbf{I}_{\ell \geq 2}$ ) is the contribution of low-energy  $\ell < 2$  ( $\ell \geq 2$ ) partial waves, and  $\mathbf{I}_H$  represents the high-frequency part in which no partial wave decomposition is performed. Extracting from  $\mathbf{I}_H$  its leading low energy behavior, one can write

$$\mathbf{I}_H(s, t) = (s^3 + u^3 C_{su}) \mathbf{H}_\Lambda + \mathbf{R}_H, \quad (3.14)$$

where  $\mathbf{H}_\Lambda$  are constants, which can be expressed as integrals over high-energy  $\pi$ - $\pi$  total cross sections, and the remainder behaves at low energies as

$$\mathbf{R}_H = O([p/\Lambda]^8). \quad (3.15)$$

The low-energy high-angular-momentum part  $\mathbf{I}_{\ell \geq 2}$  is also suppressed to  $O(p^8)$ , reflecting the leading behavior of the absorptive part  $\mathbf{A}_{\ell \geq 2}$  in the chiral limit and the fact that the corresponding dispersion integral (3.10) extends over a finite interval  $x \in [4M_\pi^2, \Lambda^2]$ . Hence, it remains to concentrate on the low-energy low-angular-momentum part  $\mathbf{I}_{\ell < 2}$ . Using Eq. (3.11), one easily checks the identity

$$\begin{aligned} \mathbf{I}_{\ell < 2} = & \Phi(s, t, u) - C_{st} \left\{ \Phi_+(t) + \frac{s-u}{t-4M_\pi^2} \Phi_-(t) \right\} \\ & + (4M_\pi^2 - 2t)(s^2 + u^2 C_{su}) \frac{1}{\pi} \int_{M_\pi^2}^{\Lambda^2} \frac{dx}{x^3} \frac{\text{Im } \Phi_-(x)}{x - 4M_\pi^2}, \end{aligned} \quad (3.16)$$

where

$$\begin{aligned} \Phi(s, t, u) = & \left\{ \Phi_+(s) + \frac{t-u}{s-4M_\pi^2} \Phi_-(s) \right\} \\ & + C_{su} \left\{ \Phi_+(u) + \frac{t-s}{u-4M_\pi^2} \Phi_-(u) \right\} \\ & + C_{st} \left\{ \Phi_+(t) + \frac{s-u}{t-4M_\pi^2} \Phi_-(t) \right\} \end{aligned} \quad (3.17)$$

and  $\Phi_\pm$  denote the following dispersion integrals over the imaginary parts of low-energy  $s$  and  $p$  waves [cf. Eq. (3.12)]:

$$\Phi_+(s) = \frac{s^3}{\pi} \int_{4M_\pi^2}^{\Lambda^2} \frac{dx}{x^3} \frac{\text{Im } \Phi_+(x)}{x-s}, \quad (3.18)$$

$$\Phi_-(s) = \frac{s^2(s-4M_\pi^2)}{\pi} \int_{4M_\pi^2}^{\Lambda^2} \frac{dx}{x^2(x-4M_\pi^2)} \frac{\text{Im } \Phi_-(x)}{x-s}.$$

One observes from Eq. (3.17) that the function  $\Phi(s, t, u)$  exhibits the full three-channel crossing symmetry. Furthermore, the second and third terms in Eq. (3.16) represent a function that is quadratic in  $s$  (at fixed  $t$ ) and symmetric under  $s$ - $u$  crossing. These terms can therefore be absorbed into the subtraction polynomial in the dispersion relations (3.10) by a suitable redefinition of (yet unknown) subtraction functions  $\mathbf{a}_+$ ,  $\mathbf{b}_-$ ,  $\mathbf{c}_+$ . Consequently, the whole amplitude  $\mathbf{F}$  can be rewritten as

$$\mathbf{F}(s, t) = \Phi(s, t, u) + \mathbf{P}(s, t, u) + O([p/\Lambda]^8), \quad (3.19)$$

where  $\mathbf{P}$  is of the form

$$\begin{aligned} \mathbf{P} = & C_{st} \left\{ \alpha_+(t) + (s-u)\beta_-(t) + (s-u)^2\gamma_+(t) \right\} \\ & + (s^3 + u^3 C_{su}) \mathbf{H}_\Lambda. \end{aligned} \quad (3.20)$$

Notice that the unspecified  $O(p^8)$  contributions in Eq. (3.19) originate both from the high-energy remainder  $\mathbf{R}_H$  (3.14) and from the low-energy higher-angular-momentum part  $\mathbf{I}_{\ell \geq 2}$ . Crossing symmetry of the scattering amplitude  $\mathbf{F}$  should hold order by order in the chiral expansion. Since the function  $\Phi$  (3.17) exhibits full crossing symmetry, it remains to impose the latter for the function  $\mathbf{P}$  (3.20). Because of the manifest  $s$ - $u$  symmetry, it is enough to require

$$\mathbf{P}(s, t, u) = C_{st} \mathbf{P}(t, s, u). \quad (3.21)$$

Neglecting  $O(p^8)$  contributions, this equation represents the necessary and sufficient condition for the complete crossing symmetry of the amplitude  $\mathbf{F}$ .

Equation (3.21) can be easily solved. Considering  $s$  and  $t$  as independent variables, one easily finds that  $\alpha_+(t)$ ,  $\beta_-(t)$ , and  $\gamma_+(t)$  should be cubic, quadratic and linear functions of  $t$ , respectively. Hence,  $\mathbf{P}(s, t, u)$  is a general crossing symmetric polynomial in the Mandelstam variables of (at most) third order. Such a polynomial contains six independent parameters (see Appendix A). Indeed, after some simple but lengthy algebra, one verifies that Eq. (3.21) leaves a six parameter freedom in the original expression (3.20) for  $\mathbf{P}$ .

It remains to rewrite the result (3.19) in terms of the single amplitude

$$A(s|tu) = A(s|ut) = \frac{32\pi}{3} \left\{ F^{(0)}(s, t, u) - F^{(2)}(s, t, u) \right\}. \quad (3.22)$$

The function  $\Phi$  gives rise to a contribution of the form (3.2) in which only the dispersion integrals of Eq. (3.6) occur. [One easily checks that  $\text{Im} T$ ,  $\text{Im} U$ , and  $\text{Im} V$  are given by Eqs. (3.4).] Furthermore, taking into account the ambiguity (3.5) in the definition of  $T$ ,  $U$ , and  $V$ , it is clear that a general crossing symmetric polynomial may be conveniently parametrized by the six independent parameters  $t_0, t_2, t_3, v_1, v_2, v_3$  as in Eqs. (3.6).

#### IV. PERTURBATIVE $\pi$ - $\pi$ AMPLITUDE AND THE EFFECTIVE INFRARED DIMENSION OF THE QUARK MASS

We are now in a position to compare the two alternative low-energy expansions of the amplitude  $A(s|tu)$  generated by chiral perturbation theory according to the two possible values of the effective dimension of the quark mass: 2, in the case of the standard  $\chi$ PT, and 1 in the case which was defined in Sec. II as improved  $\chi$ PT. Up to and including two loops, the amplitude  $A$  should be of the general form (3.2). Consequently, neglecting  $O(p^8)$  contributions, one can work with the three functions  $T, U$  and  $V$  of a single variable and decompose them as

$$T(s) = \sum_{n=0}^2 T^{(n)}(s), \quad U(s) = \sum_{n=0}^2 U^{(n)}(s), \quad (4.1)$$

$$V(s) = \sum_{n=0}^2 V^{(n)}(s),$$

where  $n$  refers to the number of loops (including tree contributions of the corresponding order). It will be shown that the amplitudes  $T, U$ , and  $V$  start to be sensitive to the effective dimension of the quark mass at leading ( $n = 0$ ), one-loop ( $n = 1$ ) and two-loop levels, respectively.

##### A. Leading $O(p^2)$ order

If the dimension of the quark mass is 2, i.e., if each power of the scalar pseudoscalar source  $\chi$  in  $\mathcal{L}_{\text{eff}}$  counts for two powers of pion momentum (mass), then the effective Lagrangian is dominated by the well-known expression

$$\mathcal{L}^{(2)} = \frac{1}{4} F_0^2 \{ \langle (D^\mu U)^\dagger (D_\mu U) \rangle + 2B_0 \langle \chi^\dagger U + U^\dagger \chi \rangle \}. \quad (4.2)$$

This formula collects all possible invariants of dimension 2. To leading order, the pion and the kaon masses read

$$\overset{\circ}{M}_\pi^2 = 2\hat{m}B_0, \quad (4.3)$$

$$\overset{\circ}{M}_K^2 = (m_s + \hat{m})B_0,$$

and the  $\pi$ - $\pi$  amplitude takes the well-known form, first given by Weinberg [15]:

$$A_{\text{lead}}(s|tu) = \frac{1}{F_0^2} (s - 2\hat{m}B_0) = \frac{1}{F_0^2} (s - \overset{\circ}{M}_\pi^2). \quad (4.4)$$

This represents the standard scenario of chiral perturbation theory. It can hardly be circumvented provided the scale of  $B_0$  is large compared to the pion mass, typically,  $B_0 \gtrsim 1$  GeV.

On the other hand, if  $B_0$  turned out to be much smaller than the GeV scale, e.g., comparable to the fundamental order parameter  $F_0$  ( $\sim 93$  MeV), then the above way of counting effective infrared dimensions would be modified. Both the quark mass and the condensate  $B_0$  should then be considered as quantities comparable to the pion mass. They should both be attributed effective infrared dimension 1, and they should both be viewed as expansion parameters. In this case, every insertion of the source  $\chi(x)$  counts as a single power of pion momentum and the formula (4.2) no longer represents the most general expression of dimension 2. Instead, the complete collection of invariants of dimension 2 now reads

$$\begin{aligned} \tilde{\mathcal{L}}^{(2)} = & \frac{1}{4} F_0^2 \{ \langle D^\mu U D_\mu U^\dagger \rangle + 2B_0 \langle \chi^\dagger U + \chi U^\dagger \rangle \\ & + A_0 \langle \chi^\dagger U \chi^\dagger U + \chi U^\dagger \chi U^\dagger \rangle + Z_0^S \langle \chi^\dagger U + U^\dagger \chi \rangle^2 \\ & + Z_0^P \langle \chi^\dagger U - \chi U^\dagger \rangle^2 + 2H_0 \langle \chi^\dagger \chi \rangle \}. \end{aligned} \quad (4.5)$$

where the tilde over the symbol  $\mathcal{L}$  here (and below) indicates the use of the modified chiral power counting. The terms containing two powers of  $\chi$  are usually included into the next-to-the-leading part  $\mathcal{L}^{(4)}$  of the effective Lagrangian. Here, they appear of the same dimension and they are expected to be of a comparable size as the standard expression (4.2). The low-energy constants  $A_0, Z_0^S$ , and  $Z_0^P$  represent appropriately subtracted zero-momentum transfer two-point functions of scalar and pseudoscalar quark densities, divided by  $F_0^2$ . These two-point functions are order parameters of spontaneous chiral symmetry breaking and, consequently, they satisfy superconvergent dispersion relations. A simple saturation of the latter with a few of the lowest massive hadronic states suggests that the dimensionless constants  $A_0$  and  $Z_0^P$  are of the order 1, say,  $A_0 \sim 1-5$ . On the other hand,  $Z_0^S$  violates the Zweig rule in the  $0^{++}$  channel and consequently it is expected to be suppressed. The parameters  $Z_0^S, Z_0^P$ , and  $A_0$  are related to the low-energy constants  $L_6, L_7$ , and  $L_8$  of the standard  $d = 4$  Lagrangian  $\mathcal{L}^{(4)}$

[3]. Expanding the latter constants in powers of  $B_0$ , one gets<sup>2</sup>

$$\begin{aligned} L_6 &= \left(\frac{F_0}{4B_0}\right)^2 \{Z_0^S + O(B_0^2)\}, \\ L_7 &= \left(\frac{F_0}{4B_0}\right)^2 Z_0^P, \\ L_8 &= \left(\frac{F_0}{4B_0}\right)^2 \{A_0 + O(B_0^2)\}, \end{aligned} \quad (4.6)$$

where  $O(B_0^2)$  terms represent divergent contributions to the two-point functions defining the divergent parts of the bare constants  $L_6, L_8$ . (The constants  $A_0, Z_0^S$ , and  $Z_0^P$  do not undergo any infinite renormalization.)

The leading order pion and kaon masses (denoted by a tilde) now read

$$\begin{aligned} \widetilde{M}_\pi^2 &= 2\hat{m}(\tilde{B} + 4\hat{m}Z_0^S) + 4\hat{m}^2 A_0, \\ \widetilde{M}_K^2 &= (m_s + \hat{m})(\tilde{B} + 4\hat{m}Z_0^S) + (m_s + \hat{m})^2 A_0. \end{aligned} \quad (4.7)$$

Here  $\tilde{B}$  stands for the dominant  $O(p)$  contribution to the  $SU(2) \times SU(2)$  quark-antiquark condensate (divided by  $F_0^2$ ) taken at  $m_u = m_d = 0$ :

$$\langle \bar{u}u \rangle_{m_u=m_d=0} = \langle \bar{d}d \rangle_{m_u=m_d=0} = -F_0^2 \tilde{B} + O(m_s^2). \quad (4.8)$$

Within the modified chiral power counting,  $\tilde{B}$  consists of two terms

$$\tilde{B} = B_0 + 2m_s Z_0^S, \quad (4.9)$$

which are both of the order  $O(p)$ . In principle, they could be of comparable size, if  $Z_0^S$  were not suppressed by the Zweig rule.

The leading contribution to the  $\pi$ - $\pi$  scattering amplitude calculated from the improved  $O(p^2)$  Lagrangian (4.5) turns out to be independent of low-energy parameters  $A_0$  and  $Z_0^P$ , and it can be expressed in term of the quark-antiquark condensate  $\tilde{B}$ ,

$$A_{\text{lead}}(s|tu) = \frac{1}{F_0^2}(s - 2\hat{m}\tilde{B}), \quad (4.10)$$

in complete analogy with the standard result (4.4). Although Eq. (4.10) and Weinberg's formula (4.4) formally coincide if one neglects Zweig-rule violation, their numerical content is rather different, because of different scales of quark-antiquark condensation in each  $\chi$ PT alternative. In Eq. (4.4),  $2\hat{m}B_0$  is the leading approximation to  $M_\pi^2$ , whereas in the improved  $\chi$ PT, the relation between the

quark-antiquark condensate and the pion mass is more subtle: Indeed, using first Eq. (4.7), formula (4.10) can be rewritten as

$$A_{\text{lead}}(s|tu) = \frac{1}{F_0^2}(s - \widetilde{M}_\pi^2) + \frac{\widetilde{M}_\pi^2}{F_0^2} \epsilon(1 + 2\zeta), \quad (4.11)$$

where

$$\epsilon = \frac{4\hat{m}^2 A_0}{\widetilde{M}_\pi^2}, \quad \zeta = \frac{Z_0^S}{A_0}. \quad (4.12)$$

Whereas in the standard  $\chi$ PT  $\epsilon$  would be a small quantity of the order  $O(p^2)$ , in the improved  $\chi$ PT,  $\epsilon$  is of order 1 and there is no reason for it to be particularly small; hence, the second term in Eq. (4.11) represents a *leading order* modification of the Weinberg's formula (4.4). ( $\zeta$  measures the Zweig rule violation in the  $0^{++}$  channel and can be expected rather small.) Using Eqs. (4.7) one may easily check that  $\epsilon$  can indeed be of order 1 for natural values of  $A_0$  (cf. footnote 2) and for reasonably small values of quark masses. Setting, for the sake of illustration,  $B_0 = 150$  MeV and  $\hat{m} = 25$  MeV, and neglecting Zweig-rule violation, one obtains  $\epsilon = 0.62$ ,  $A_0 = 4.8$ , and  $m_s \simeq 195$  MeV.

The leading-order mass formula (4.7) implies a relation between the parameter  $\epsilon$  and the quark-mass ratio  $r = m_s/\hat{m}$ :

$$\epsilon = 2 \frac{r_2 - r}{r^2 - 1}, \quad r_2 = 2 \frac{\widetilde{M}_K^2}{\widetilde{M}_\pi^2} - 1 \simeq 25.9. \quad (4.13)$$

If  $r$  decreases from its canonical leading order value  $r = r_2$ , then  $\epsilon$  increases and reaches 1 for  $r = r_1$ :

$$r_1 = 2 \frac{\widetilde{M}_K}{\widetilde{M}_\pi} - 1 \simeq 6.33. \quad (4.14)$$

Similarly, the order parameter  $B_0$  can be expressed as

$$\frac{2\hat{m}B_0}{\widetilde{M}_\pi^2} = 1 - [1 + (r + 2)\zeta]\epsilon. \quad (4.15)$$

This ratio decreases from its canonical value 1 down to zero, as  $r$  decreases from  $r = r_2$  to  $r = r_{\text{crit}}(\zeta) \gtrsim r_1$ , for which  $B_0$  vanishes. Notice that stability of the massless QCD vacuum under perturbation by small quark masses implies  $B_0 \geq 0$ .

## B. Next to the leading $O(p^3)$ contribution

In the improved chiral perturbation theory, the leading order Lagrangian  $\tilde{\mathcal{L}}^{(2)}$  is followed by a *dimension-3 term*  $\tilde{\mathcal{L}}^{(3)}$ , which contributes at the tree level before one-loop contributions of dimension 4 start to appear.  $\tilde{\mathcal{L}}^{(3)}$  reads

$$\begin{aligned} \tilde{\mathcal{L}}^{(3)} &= \frac{1}{4} F_0^2 \{ \xi \langle D_\mu U^\dagger D^\mu \chi + D_\mu \chi^\dagger D^\mu U \rangle \\ &\quad + \rho_1 \langle (\chi^\dagger U)^3 + (\chi U^\dagger)^3 \rangle + \rho_2 \langle \chi^\dagger \chi (\chi^\dagger U + U^\dagger \chi) \rangle \\ &\quad + \rho_3 \langle (\chi^\dagger U)^2 - (\chi U^\dagger)^2 \rangle \langle \chi^\dagger U - \chi U^\dagger \rangle + \dots \}. \end{aligned} \quad (4.16)$$

<sup>2</sup>The order of magnitude estimate  $A_0 \sim 1 - 5$  is compatible with the standard  $\chi$ PT estimates. Taking  $A_0 \sim 5$ , and using the standard value  $B_0 \sim 1.2$  GeV, the  $A_0$  contribution to  $L_8$  in Eq. (4.6) becomes  $1.6 \times 10^{-3}$ , which is consistent with the standard  $\chi$ PT measurement of  $L_8$  [3].

The dots stand for terms that violate the Zweig rule in a nonanomalous channel. Notice that (4.16) differs in its first term from the expression given for  $\tilde{\mathcal{L}}^{(3)}$  in Ref. [6]. The two forms of  $\tilde{\mathcal{L}}^{(3)}$  are equivalent: They are related by a simple redefinition of the Goldstone boson field  $U$ . The low-energy constants  $\xi$  and  $\rho_i$  are finite — there are no divergences of dimension 3.  $\tilde{\mathcal{L}}^{(3)}$  induces a shift in the pion mass:

$$\delta M_\pi^2 = \epsilon \widetilde{M}_\pi^2 (9\lambda_1 + \lambda_2), \quad (4.17)$$

where

$$\lambda_i = \frac{\hat{m}\rho_i}{4A_0} \quad (4.18)$$

are dimensionless parameters of order  $O(M_\pi)$ . Similarly, the leading  $\pi$ - $\pi$  amplitude receives a constant  $d = 3$  contribution

$$\delta \tilde{A}(s|tu) = \epsilon \frac{\widetilde{M}_\pi^2}{3F_0^2} (81\lambda_1 + \lambda_2). \quad (4.19)$$

Finally, the first term in  $\tilde{\mathcal{L}}^{(3)}$  is responsible for splitting of the decay constants  $F_\pi, F_K, F_\eta$ . Eliminating the low-energy parameter  $\xi$ , one obtains, to that order

$$\frac{F_\pi^2}{F_0^2} = 1 + \frac{2}{r-1} \left( \frac{F_K^2}{F_\pi^2} - 1 \right). \quad (4.20)$$

It is convenient to collect all  $d = 2$  and  $d = 3$  contributions, and to express the resulting tree amplitude in the form (3.1):

$$A_{\text{tree}}(s|tu) = \frac{1}{3F_\pi^2} [\alpha M_\pi^2 + \beta(3s - 4M_\pi^2)] + \frac{M_\pi^2}{3F_\pi^2} \delta\alpha, \quad (4.21)$$

where  $M_\pi$  and  $F_\pi$  denote the *experimental* (charged) pion mass and decay constant.<sup>3</sup> The parameters  $\alpha$  and  $\beta$  read

$$\frac{\alpha}{\beta} = 1 + 3\epsilon(1 + 2\zeta), \quad \beta = \frac{F_\pi^2}{F_0^2}, \quad (4.22)$$

whereas  $\delta\alpha = \delta\alpha_3 + \delta\alpha_4$  describes small  $O(p^3)$  and  $O(p^4)$  corrections.  $\delta\alpha$  arises from the genuine  $O(p^3)$  contribution (4.19) of  $\tilde{\mathcal{L}}^{(3)}$  to the  $\pi - \pi$  amplitude and from the introduction of the physical mass  $M_\pi$  into the formula (4.21). Using Eqs. (4.17) and (4.19), the  $O(p^3)$  constant  $M_\pi^2 \delta\alpha_3$  can be expressed in terms of the parameters  $\lambda_1$  and  $\lambda_2$  of  $\tilde{\mathcal{L}}^{(3)}$ :

$$M_\pi^2 \delta\alpha_3 = \epsilon \beta \widetilde{M}_\pi^2 [72\lambda_1 - (27\lambda_1 + 3\lambda_2)\epsilon(1 + 2\zeta)]. \quad (4.23)$$

The remaining term  $M_\pi^2 \delta\alpha_4$  accounts for the  $O(p^4)$  and higher contributions to  $M_\pi^2$ . One has

$$M_\pi^2 \delta\alpha_4 = -\beta \Delta M_\pi^2 [1 + 3\epsilon(1 + 2\zeta)], \quad (4.24)$$

where

$$\Delta M_\pi^2 = M_\pi^2 - \widetilde{M}_\pi^2 - \delta M_\pi^2 \quad (4.25)$$

represents the  $O(p^4)$  difference between the physical value and the tree approximation of the pion mass squared.

The results of standard  $\chi$ PT are reproduced by setting  $\epsilon = \zeta = 0$  in the previous equations; i.e.,  $r = r_2 \simeq 25.9$ . In this case,  $\widetilde{M}_\pi^2$  reduces to  $M_\pi^2$  [Eq. (4.3)], and  $\alpha = \beta \simeq 1$ . The improved  $\chi$ PT still requires  $\beta \simeq 1$ , but  $\alpha$  is now allowed and expected to be considerably larger, since  $\epsilon$  is now an order-1 quantity. In fact, the vacuum stability conditions mentioned above imply that for a given quark mass ratio  $r$  [lying between  $r_1$  and  $r_2$ —cf. Eqs. (4.13) and (4.14)], the Zweig-rule-violating parameter  $\zeta = Z_0^S/A_0$  should satisfy

$$0 \leq \zeta \leq \zeta_{\text{crit}}(r) = \frac{1}{2} \frac{r - r_1}{r_2 - r} \frac{r + r_1 + 2}{r + 2}. \quad (4.26)$$

Using these bounds in Eq. (4.22), one obtains a rather narrow band of allowed values in the plane defined by the ratio  $\alpha/\beta$  and  $r$ . This band is shown in Fig. 1.

It is straightforward to rewrite the above result in terms of the amplitudes  $T$ ,  $U$ , and  $V$ . The tree contribution to these amplitudes simply reads

$$T^{(0)}(s) = (\hat{\alpha} + \delta\hat{\alpha})M_\pi^2, \quad U^{(0)}(s) = 0, \quad V^{(0)}(s) = 9\hat{\beta}, \quad (4.27)$$

where

$$\hat{\alpha} \equiv \frac{\alpha}{96\pi F_\pi^2}, \quad \hat{\beta} \equiv \frac{\beta}{96\pi F_\pi^2} \quad (4.28)$$

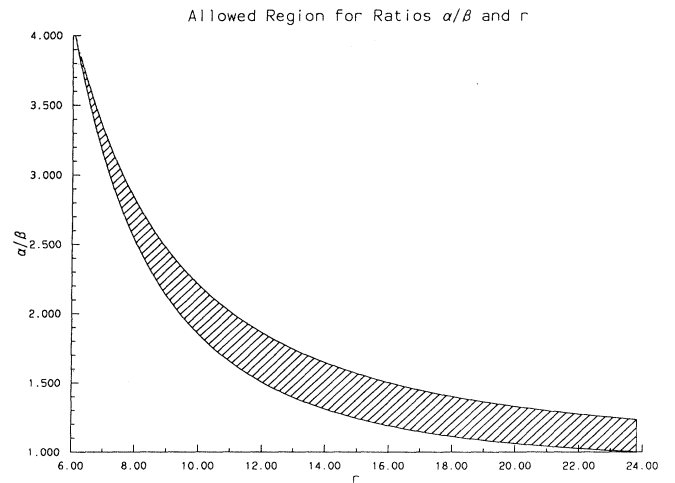


FIG. 1. The region of allowed values for the ratios  $\alpha/\beta$  and  $m_s/\hat{m}$  lies between the two curves shown.

<sup>3</sup>In practice,  $M_\pi = 139.6$  MeV and  $F_\pi = 93.1$  MeV will be identified with the corresponding theoretical expressions up to and including the highest order of  $\chi$ PT considered.

and likewise for  $\delta\hat{\alpha}$ . Our main task is to use all available experimental information to measure  $\alpha, \beta$  and, indirectly, the quark mass ratio  $r$ .

### C. One loop $O(p^4)$ order

Let  $\mathcal{L}_{nm}$  denote an invariant entering the effective Lagrangian, that contains  $n$  powers of covariant derivatives  $D$  and  $m$  insertions of the scalar-pseudoscalar source  $\chi$ . [For simplicity, the expansion coefficients  $\ell^{nm}$  of Eq. (2.7) are included in  $\mathcal{L}_{nm}$ .] In the standard chiral perturbation theory the  $d = 4$  part of the effective Lagrangian can be written as

$$\mathcal{L}^{(4)} = \sum_{n+2m=4} \mathcal{L}_{nm}. \quad (4.29)$$

$$\begin{aligned} \mathcal{L}_{40} = & L_1 \langle D_\mu U^\dagger D^\mu U \rangle^2 + L_2 \langle D_\mu U^\dagger D_\nu U \rangle \langle D^\mu U^\dagger D^\nu U \rangle + L_3 \langle D_\mu U^\dagger D^\mu U D_\nu U^\dagger D^\nu U \rangle \\ & - iL_9 \langle F_{\mu\nu}^R D^\mu U D^\nu U^\dagger + F_{\mu\nu}^L D^\mu U^\dagger D^\nu U \rangle + L_{10} \langle U^\dagger F_{\mu\nu}^R U F^{L,\mu\nu} \rangle + H_1 \langle F_{\mu\nu}^R F^{R,\mu\nu} + F_{\mu\nu}^L F^{L,\mu\nu} \rangle. \end{aligned} \quad (4.31)$$

The meaning and renormalization of low-energy constants in Eq. (4.31) are independent of the symmetry breaking sector and, in particular, of the infrared dimension of the quark mass. The remaining  $B_0$ -independent terms in Eq. (4.30), cf.  $\mathcal{L}_{22}$  and  $\mathcal{L}_{04}$ , are absent from the expression for  $\mathcal{L}^{(4)}$ : With quark mass of dimension 2, these terms would count as  $O(p^6)$  and  $O(p^8)$ , respectively. On the other hand, all terms but  $\mathcal{L}_{40}$  contained in  $\mathcal{L}^{(4)}$  are already included either in  $\tilde{\mathcal{L}}^{(2)}$  or in  $\tilde{\mathcal{L}}^{(3)}$ . Consequently,  $\tilde{\mathcal{L}}^{(2)} + \tilde{\mathcal{L}}^{(3)} + \tilde{\mathcal{L}}^{(4)}$  not only encompasses all terms of the standard  $\mathcal{L}^{(2)} + \mathcal{L}^{(4)}$  but, in addition, it contains new terms of the type  $\tilde{\mathcal{L}}^{(3)}$ ,  $\mathcal{L}_{22}$ , and  $\mathcal{L}_{04}$ . This phenomenon is general. Order by order, the improved  $\chi$ PT contains the standard perturbation theory as a special case: It contains more parameters and it could well fit the experimental data even when the standard  $\chi$ PT fails.

The one-loop contribution to the  $\pi$ - $\pi$  amplitude  $A(stu)$  has been worked out within the standard chiral perturbation theory in Refs. [2,3]. The result can be expressed in terms of four constants:  $\alpha = \beta$  (close to 1), the shift  $\delta\alpha_4$  ( $\delta\alpha_3 = 0$  in this case) introduced in Eqs. (4.21), and two linear combinations of the renormalized constants  $L_1, L_2$ , and  $L_3$ . In the improved  $\chi$ PT, the one-loop  $O(p^4)$  amplitude contains, in addition, two parameters that arise from the new terms  $\mathcal{L}_{22}$  and  $\mathcal{L}_{04}$  in  $\tilde{\mathcal{L}}^{(4)}$ . Working with the amplitudes  $T, U, V$  [the formula (3.2) is valid up to and including two loops], one may obtain a closed form for the one-loop amplitude, which encompasses both alternatives of chiral perturbation theory.

Let  $\varphi_a^{(d)}(s)$  denote the effective dimension- $d$  contribution to the real part of the partial wave amplitude  $f_a(s)$ , ( $a = 0, 1, 2$ ), introduced in Sec. III B:

$$\text{Re } f_a(s) = \sum_{d \geq 2} \varphi_a^{(d)}. \quad (4.32)$$

It contains all counterterms that are needed to renormalize one-loop contributions generated by  $\mathcal{L}^{(2)}$ . If the dimension of the quark mass is 1, one-loop renormalization gets modified in two respects: (i) The effective dimension of a term  $\mathcal{L}_{nm}$  is  $d = n + m$  instead of  $d = n + 2m$ , and (ii)  $B_0$  is now a (small) expansion parameter of dimension 1. It follows, in particular, that renormalization has to be performed order by order in  $B_0$ . The modified  $d = 4$  part of  $\mathcal{L}_{\text{eff}}$  then reads

$$\tilde{\mathcal{L}}^{(4)} = \sum_{n+m=4} \mathcal{L}_{nm} + B_0 (\mathcal{L}_{21} + \mathcal{L}_{03}) + B_0^2 \mathcal{L}_{02}. \quad (4.30)$$

The last two counterterms are needed to renormalize the  $B_0$ -dependent part of one-loop divergences generated by  $\tilde{\mathcal{L}}^{(2)}$ . Terms that are contained both in  $\mathcal{L}^{(4)}$  and in  $\tilde{\mathcal{L}}^{(4)}$  are merely made with four derivatives [3]:

From Eqs. (4.27) one finds

$$\begin{aligned} \varphi_0^{(2)}(s) &= 6\hat{\beta}(s + \kappa_0), \\ \varphi_1^{(2)}(s) &= \hat{\beta}(s - 4M_\pi^2), \\ \varphi_2^{(2)}(s) &= -3\hat{\beta}(s + \kappa_2), \end{aligned} \quad (4.33)$$

where

$$\kappa_0 \equiv \left( \frac{5\alpha}{6\beta} - \frac{4}{3} \right) M_\pi^2, \quad \kappa_2 \equiv \left( -\frac{2\alpha}{3\beta} - \frac{4}{3} \right) M_\pi^2. \quad (4.34)$$

Similarly, the real parts at the  $O(p^3)$  level are

$$\varphi_0^{(3)} = 5M_\pi^2 \delta\alpha_3, \quad \varphi_1^{(3)} = 0, \quad \varphi_2^{(3)} = -2M_\pi^2 \delta\alpha_3, \quad (4.35)$$

where  $\delta\alpha_3$  is given by Eq. (4.23). For  $d > 3$ , the real parts are no longer defined by the tree amplitude alone. The  $O(p^d)$  contribution to the imaginary part of the partial wave amplitudes  $\text{Im } f_a^{(d)}(s)$  can be expressed for  $s > 4M_\pi^2$  through elastic unitarity:

$$\text{Im } f_a^{(d)}(s) = \sqrt{\frac{s - 4M_\pi^2}{s}} \sum_{d_1+d_2=d} \varphi_a^{(d_1)}(s) \varphi_a^{(d_2)}(s). \quad (4.36)$$

This result is an exact property of  $\chi$ PT amplitudes for  $4 \leq d < 8$ .

The one-loop level contains  $d = 4$ ,  $d = 5$ , and  $d = 6$  contributions to the scattering amplitude  $A(s|tu)$ . In the following, we shall merely concentrate on the leading  $O(p^4)$  part. The corresponding components of the functions,  $T, U, V$ ,<sup>4</sup> will be denoted as  $T_{\text{lead}}^{(1)}(s)$ ,  $U_{\text{lead}}^{(1)}(s)$ , and  $V_{\text{lead}}^{(1)}(s)$ . The discontinuities of these functions are given by the  $O(p^4)$  absorptive parts  $\text{Im } f_a^{(4)}$ , following

Eqs. (3.4). Hence, the  $O(p^4)$  one-loop amplitudes  $T, U, V$  can be written as

$$\begin{aligned} T_{\text{lead}}^{(1)}(s) &= \frac{1}{3} \{ [\varphi_0^{(2)}(s)]^2 + 2[\varphi_2^{(2)}(s)]^2 \} L(s, \mu^2) \\ &\quad + \alpha_4(\mu^2) + \alpha_0(\mu^2)s^2, \\ U_{\text{lead}}^{(1)}(s) &= \frac{1}{2} \{ 2[\varphi_0^{(2)}(s)]^2 - 5[\varphi_2^{(2)}(s)]^2 \} L(s, \mu^2), \\ V_{\text{lead}}^{(1)}(s) &= \frac{27}{2} \frac{[\varphi_1^{(2)}(s)]^2}{s - 4M_\pi^2} L(s, \mu^2) + \beta_2(\mu^2) + \beta_0(\mu^2)s, \end{aligned} \quad (4.37)$$

where  $L(s, \mu^2)$  is the loop integral subtracted at the point  $s = -\mu^2$ :

$$L(s, \mu^2) \equiv \frac{s + \mu^2}{\pi} \int_{4M_\pi^2}^{\infty} \frac{dx}{x + \mu^2} \frac{1}{x - s} \sqrt{\frac{x - 4M_\pi^2}{x}}. \quad (4.38)$$

The constants  $\alpha_n(\mu^2)$  and  $\beta_n(\mu^2)$  behave in the chiral limit as  $M_\pi^n$ . They describe the most general polynomial part of  $T, U$ , and  $V$ , which is  $O(p^4)$  and takes into account the freedom (3.5). These constants represent renormalized tree contributions of the  $d = 4$  part of  $\mathcal{L}_{\text{eff}}$ . Their dependence on the subtraction point  $\mu^2$  can be determined by demanding that the scattering amplitude  $A(stu)$  be  $\mu^2$  independent. Following Appendix B, this requirement is equivalent to the conditions

$$\begin{aligned} \frac{\partial}{\partial \mu^2} T^{(1)}(s) &= \delta T(s), & \frac{\partial}{\partial \mu^2} U^{(1)}(s) &= \delta U(s), \\ \frac{\partial}{\partial \mu^2} V^{(1)}(s) &= \delta V(s), \end{aligned} \quad (4.39)$$

where  $\delta T, \delta U$ , and  $\delta V$  are of the general form (3.5). Taking into account the  $s$  independence of  $(\partial/\partial \mu^2)L(s, \mu^2)$  and  $L(0, \mu^2) = -L(-\mu^2, 0)$ , the solution of Eqs. (4.39) can be easily found:

$$\begin{aligned} \alpha_0(\mu^2) &= \alpha_0(0) + 18\hat{\beta}^2 L(-\mu^2), \\ \beta_0(\mu^2) &= \beta_0(0), \\ \alpha_4(\mu^2) &= \alpha_4(0) + (11\hat{\alpha}^2 - 32\hat{\beta}^2)M_\pi^4 L(-\mu^2), \\ \beta_2(\mu^2) &= \beta_2(0) + 18\hat{\beta}(5\hat{\alpha} - 2\hat{\beta})M_\pi^2 L(-\mu^2). \end{aligned} \quad (4.40)$$

In these equations we have denoted

$$\begin{aligned} L(s) \equiv L(s, \mu^2 = 0) &= \frac{1}{\pi} \left[ 2 + \sigma \ln \left( \frac{\sigma - 1}{\sigma + 1} \right) \right], \\ \sigma &= \sqrt{1 - \frac{4M_\pi^2}{s}}. \end{aligned} \quad (4.41)$$

<sup>4</sup>Notice that  $O(p^N)$  terms in  $V$  contribute to the scattering amplitude  $A$  of Eq. (3.2) as  $O(p^{N+2})$ .

In the following we shall work at  $\mu^2 = 0$ .

The constants  $\alpha_0$  and  $\beta_0$  are related to the low-energy parameters  $L_1, L_2$ , and  $L_3$  which occur in the expression (4.31) for  $\mathcal{L}_{40}$ . One gets

$$\begin{aligned} \alpha_0(0) &= \frac{1}{4\pi F_0^4} [L_1^r + L_2^r + \frac{1}{2}L_3 - \frac{1}{4}\nu(\bar{\mu}^2)], \\ \beta_0(0) &= \frac{3}{8\pi F_0^4} (L_2^r - 2L_1^r - L_3) + \frac{1}{1024\pi^3 F_0^4}, \end{aligned} \quad (4.42)$$

where

$$\nu(\bar{\mu}^2) = \frac{1}{32\pi^2} \left[ \ln \frac{M_\pi^2}{\bar{\mu}^2} + \frac{1}{8} \ln \frac{M_K^2}{\bar{\mu}^2} + \frac{9}{8} \right], \quad (4.43)$$

and  $\bar{\mu}^2$  denotes the renormalization scale introduced in Ref. [3]. The renormalized constants  $L_1^r, L_2^r$  are  $\bar{\mu}^2$ -dependent, whereas  $L_3$  and  $L_2^r - 2L_1^r$  are not. Furthermore, the combination  $L_2^r - 2L_1^r$  should be suppressed by the Zweig rule or in the large  $N_c$  limit. Notice that the constant  $\beta_0$  is independent both of  $\mu^2$  and of  $\bar{\mu}^2$ . The interpretation of the remaining two constants  $\alpha_4$  and  $\beta_2$  depends on the effective dimension of the quark mass. In the standard chiral perturbation theory, these constants can be expressed in terms of the shifts of the pion mass and decay constant, as calculated within  $SU(2) \times SU(2)$  perturbation theory [2]. In the improved  $\chi$ PT,  $\alpha_4(0)$  and  $\beta_2(0)$  are independent parameters, which describe respective contributions of new terms  $\mathcal{L}_{04}$  and  $\mathcal{L}_{22}$  in the  $O(p^4)$  effective Lagrangian  $\tilde{\mathcal{L}}^{(4)}$ . The explicit relationship between  $\alpha_4(0), \beta_2(0)$  and the low-energy parameters of  $\tilde{\mathcal{L}}^{(4)}$  is of no direct use in the present paper, and it will be given elsewhere.

Concluding this section, it is worth noting that the low-energy theorem of Sec. III considerably simplifies the calculation of two-loop contributions to  $A(stu)$ : For  $d < 8$ , all  $O(p^d)$  terms can be obtained by a straightforward combination of Eqs. (3.2) and (3.4) with the unitarity condition (4.36). Up to and including two loops, the  $\chi$ PT expansion of the  $\pi$ - $\pi$  scattering amplitude can be viewed as an iteration of the Roy-type Eqs. (3.7a) and (3.7b). The corresponding polynomials  $P_a(s)$  appearing at a given order  $O(p^d)$  are then defined in terms of the renormalized low-energy constants of the Lagrangians  $\mathcal{L}^{(d)}$  or  $\tilde{\mathcal{L}}^{(d)}$ , according to the effective dimension of the quark mass being, respectively, 2 or 1.

## V. DETERMINATION OF PARAMETERS OF $\mathcal{L}_{\text{EFF}}$ FROM $\pi$ - $\pi$ SCATTERING DATA

Suppose one has enough experimental information to perform the program formulated in Sec. III and to reconstruct the low-energy amplitude  $A(stu)$ . Let us call the result of this reconstruction  $A_{\text{expt}}(sttu)$  and the corresponding  $T, U, V$  amplitudes given by Eqs. (3.4)  $T_{\text{expt}}, U_{\text{expt}}$ , and  $V_{\text{expt}}$ , respectively. We would like to compare the experimental amplitude  $A_{\text{expt}}$  with the theoretical amplitude  $A_{\text{th}}$  given in Sec. IV in a whole low-energy domain of the  $s$ - $t$ - $u$  plane including the unphysical re-

tion. Such a comparison should lead to a detailed fit, which in turn should provide a rather precise determination of low-energy constants entering  $A_{\text{th}}$ . In particular, we would like to measure the parameter  $\alpha$  and, in this way, let Nature tell us whether it prefers a quark mass of effective dimension 1 or 2. The theorem proved in Sec. III considerably simplifies the above task: Neglecting  $O(p^8)$  contributions, the equation

$$A_{\text{expt}}(s|tu) - A_{\text{th}}(s|tu) = 0, \tag{5.1}$$

which is supposed to hold in a crossing symmetric domain of the Mandelstam plane, is actually equivalent to a set of three *single-variable* equations:

$$\begin{aligned} T_{\text{expt}}(s) - T_{\text{th}}(s) &= \delta T(s), \\ U_{\text{expt}}(s) - U_{\text{th}}(s) &= \delta U(s), \\ V_{\text{expt}}(s) - V_{\text{th}}(s) &= \delta V(s), \end{aligned} \tag{5.2}$$

valid in an interval of  $s$ . The functions  $\delta T(s)$ ,  $\delta U(s)$ , and  $\delta V(s)$  are the arbitrary and irrelevant polynomials given by Eq. (3.5). In this section, we will analyze Eqs. (5.2). Hereafter we systematically set  $M_\pi^2 = 1$ .

**A. One-loop precision**

The functions  $T_{\text{expt}}$ ,  $U_{\text{expt}}$ , and  $V_{\text{expt}}$  are given by Eqs. (3.6). Up to and including (one-loop) order  $O(p^4)$ , the theoretical amplitude reads

$$T_{\text{th}} = T^{(0)} + T_{\text{lead}}^{(1)} \tag{5.3}$$

(and likewise for  $U$  and  $V$ ), where the tree and leading one-loop contributions are presented in Eqs. (4.27) and (4.37), respectively. We shall concentrate on real parts of Eqs. (5.2).

Let us denote the partial wave integrals appearing in Eqs. (3.6) as

$$\phi_a(s) = \frac{s^3}{\pi} \int_4^{\Lambda^2} \frac{dx}{x^3} \frac{\text{Im } f_a(x)}{x-s}, \quad a = 0, 2 \tag{5.4}$$

$$\phi_1(s) = \frac{s^2}{\pi} \int_4^{\Lambda^2} \frac{dx}{x^2} \frac{1}{x-4} \frac{\text{Im } f_1(x)}{x-s},$$

It is convenient to take linear combinations of the Eqs. (5.2) for  $T$  and  $U$  and isolate the contributions of  $I = 0$  and  $I = 2$   $s$  waves. The resulting equations can be written as ( $a = 0, 2$ )

$$\phi_a(s) = \frac{\hat{\beta}^2 N_a}{6\pi} (s + \kappa_a)^2 D(s) + p_a(s), \tag{5.5}$$

where

$$N_0 = 36, \quad N_2 = 9, \tag{5.6}$$

and ( $w \equiv |1 - 4/s|^{1/2}$ ),

$$D(s) \equiv 6\pi \text{Re } L(s),$$

$$D(s) = 12 + 6w \ln \left| \frac{1-w}{1+w} \right|, \quad s \leq 0, \quad s \geq 4, \tag{5.7}$$

$$D(s) = 12 - 12w \arctan w^{-1}, \quad 0 \leq s \leq 4.$$

The  $p_a(s)$  are two third-order polynomials, whose coefficients are given in terms of (i) three constants  $t_i$  [cf. the first of Eqs. (3.6)], (ii) the parameters  $\alpha, \beta, \alpha_0(0)$  and  $\alpha_4(0)$  defined in terms of  $\mathcal{L}_{\text{eff}}$ , and (iii) the irrelevant five constants that characterize the polynomial ambiguity (3.5). The explicit expression for the coefficients of  $p_a(s)$  can be easily read off from Eqs. (3.6), (4.27), and (4.37). Similarly, the  $V$  equation (5.2) can be written as

$$\phi_1(s) = \frac{\hat{\beta}^2}{6\pi} (s-4)D(s) + q(s), \tag{5.5'}$$

where  $q(s)$  is now a second-order polynomial with coefficients given by linear combinations of three parameters  $v_i$  [cf. the last of Eqs. (3.4)], the  $\mathcal{L}_{\text{eff}}$  parameters  $\beta_0(0)$  and  $\beta_2(0)$  and the irrelevant constants  $y_i$ . For small  $s$ , the function  $D(s)$  behaves as

$$D(s) = s + \frac{1}{10}s^2 + O(s^3). \tag{5.8}$$

On the other hand, the functions  $\phi_a(s)$  and  $\phi_1(s)$  defined in (5.4) behave as  $O(s^3)$  and  $O(s^2)$ , respectively. The polynomials  $p_a(s)$  and  $q(s)$  should be such to ensure this small- $s$  behavior on the right-hand sides of Eqs. (5.5) and (5.5'). Using (5.8), one easily finds ( $a = 0, 2$ )

$$p_a(s) = \frac{\hat{\beta}^2 N_a}{6\pi} \left\{ -\kappa_a^2 s - \frac{1}{10} \kappa_a (\kappa_a + 20) s^2 + \tau_a s^3 \right\}, \tag{5.9}$$

$$q(s) = \frac{\hat{\beta}^2}{6\pi} \left\{ -s(s-4) + \tau_1 s^2 \right\},$$

where  $\tau_0, \tau_1, \tau_2$  are three yet undetermined parameters. Equations (5.5) and (5.5') now take the form ( $a = 0, 2$ )

$$\begin{aligned} \phi_a(s) = \frac{\hat{\beta}^2 N_a}{6\pi} \left\{ s^2 D(s) + 2s[D(s) - s]\kappa_a \right. \\ \left. + [D(s) - s - \frac{1}{10}s^2]\kappa_a^2 + \tau_a s^3 \right\}, \end{aligned} \tag{5.10}$$

$$\phi_1(s) = \frac{\hat{\beta}^2}{6\pi} \left\{ (s-4)[D(s) - s] + \tau_1 s^2 \right\}.$$

Once the experimental phase shifts are known, one can compute the integrals  $\phi(s)$  on left-hand side of Eq. (5.10) and fit them with the corresponding right-hand side. The parameters of the fit are  $\alpha, \beta, \tau_0, \tau_1, \tau_2$ . At this stage, one does not need to know the subtraction constants  $t_i$  and  $v_i$

in the dispersion relations (3.6). The latter are needed, however, if one wants to measure the four parameters of  $\mathcal{L}^{(4)}$ , namely,  $\alpha_0(0)$ ,  $\beta_0(0)$ ,  $\delta\hat{\alpha} + \alpha_4(0)$ , and  $\beta_2(0)$ . [Remember that the parameters  $\alpha_0(0)$  and  $\beta_0(0)$  determine the two linear combinations (4.42) of the low-energy constants  $L_1, L_2$ , and  $L_3$  that appear in the  $\mathcal{L}_{40}$  part (4.31) of  $\mathcal{L}_{\text{eff}}$ .] Indeed, comparing coefficients of polynomials on both sides of Eqs. (5.9), one gets 11 linear relations among the “experimental” constants  $t_0, t_2, t_3, v_1, v_2, v_3$ , the four parameters of  $\mathcal{L}_{\text{eff}}$  mentioned above, and the irrelevant five constants  $x, y_0, y_1, y_2, y_3$ . Eliminating the latter, one can express the four  $\mathcal{L}_{\text{eff}}$  parameters as

$$\alpha_0(0) = t_2 - \frac{\hat{\beta}^2}{10\pi} \{2\kappa_0(\kappa_0 + 20) + \kappa_2(\kappa_2 + 20)\}, \quad (5.11a)$$

$$\beta_0(0) = v_2 + \frac{9\hat{\beta}^2}{\pi}(1 - 8\tau_0 + 5\tau_2) + \frac{3\hat{\beta}^2}{40\pi} \{8\kappa_0(\kappa_0 + 20) - 5\kappa_2(\kappa_2 + 20)\},$$

and

$$\delta\hat{\alpha} + \alpha_4(0) = t_0 - \hat{\alpha} - \frac{4\hat{\beta}^2}{3\pi}(2\kappa_0^2 + \kappa_2^2) \quad (5.11b)$$

$$\beta_2(0) = v_1 - 9\hat{\beta} + \frac{21\hat{\beta}^2}{20\pi} \{5\kappa_2^2 - 8\kappa_0^2\} + \frac{6\hat{\beta}^2}{\pi} \{5(\kappa_2 - 2\tau_2) - 8(\kappa_0 - 2\tau_0)\}.$$

The remaining two equations do not involve any parameter of  $\mathcal{L}_{\text{eff}}$  to be determined. They read

$$t_3 = -\frac{\hat{\beta}^2}{\pi}(2\tau_0 + \tau_2), \quad (5.12)$$

$$v_3 = \frac{9\hat{\beta}^2}{4\pi}(1 - 8\tau_0 + 5\tau_2 - \tau_1).$$

The two Eqs. (5.12) should be merely expected to measure the strength of neglected two-loop and  $\tilde{\mathcal{L}}^{(6)}$  contributions, rather than represent a true constraint on the fit based on Eqs. (5.10).

### B. Fits to Roy-type equations (3.7a) and (3.7b)

In order to reconstruct the amplitude  $A_{\text{expt}}(s|tu)$ , one needs a complete set of pion-pion phase shifts  $\delta_a(s)$ , ( $a = 0, 1, 2$ ). (By complete we mean that they extend in energy from the threshold to  $\Lambda \lesssim 1$  GeV for all three isospins and are dense enough in the interval to allow adequate numerical evaluation of our dispersion integrals.)

There exists only one complete set of pion-pion scattering phase shifts (extrapolated from experimental data<sup>5</sup>)

that has been published in numerical form, namely that appearing in the paper of Froggatt and Petersen [17]. They provide values for  $\delta_a(s)$ , without quoted errors, at 20-MeV energy intervals in  $4M_\pi^2 < s < \Lambda^2$ , for  $a = 0, 1, 2$ . The phase shifts  $\delta_a$  come from an analysis following that of Basdevant, Froggatt, and Petersen [23], which employs a truncated set of twice-subtracted Roy equations, makes a particular choice of parametrization for  $f_a$  (fixing the  $I = 0$  scattering length,  $a_0$ ) and uses a Regge-type model for estimating the high-energy contributions to the dispersion integrals. Data were taken from the Estabrooks-Martin analysis [27] of the CERN-Munich experiment on  $\pi N \rightarrow \pi\pi N$  [28]. Although Basdevant, Froggatt, and Petersen [23] present graphical results for several choices of values of  $a_0$  in their work, numerical results are only presented in the subsequent paper of Froggatt and Petersen [17], and only for the unique choice  $a_0 = 0.3$ .

We first check to what extent the Froggatt-Petersen phases satisfy the version of the Roy equations set forth in Sec. III B. To this end, we compute the integrals on the right-hand side of Eqs. (3.7a) and (3.7b), using the  $\delta_a$  from Froggatt and Petersen. Calling the result  $\text{Re}f_a^{\text{RHS}}(s)$ , we then determine the parameters  $t_i, v_i$  by minimizing

$$\sum_a \sum_i [\text{Re}f_a^{\text{LHS}}(s_i) - \text{Re}f_a^{\text{RHS}}(s_i)]^2, \quad (5.13)$$

where  $\text{Re}f_a^{\text{LHS}}$  is the real part of  $f_a$  determined directly (via unitarity) from  $\delta_a$ . This is not a proper  $\chi^2$  fit, since no uncertainties can be included; consequently, no uncertainties can be quoted for the resulting constants. We find, however, that the values for experimentally determined constants are stable for reasonable variations in the energy interval used for the fit (see Table I). The fit over the largest range,  $4 < s < 25$ , is excellent:  $\text{Re}f_a^{\text{RHS}}$  and  $\text{Re}f_a^{\text{LHS}}$  agree to 1% over nearly all the interval, the sum in Eq. (5.13) being  $\sim 10^{-4}$  for 63 data points. We see no need to present the results graphically:  $\text{Re}f_a^{\text{RHS}}$  and  $\text{Re}f_a^{\text{LHS}}$  would be indistinguishable. Instead, the val-

TABLE I. Parameters resulting from fitting Eqs. (3.7a) and (3.7b).

Parameter	Energy range for fit (MeV)		
	300–580	300–640	300–700
Using phase shifts of Froggatt and Petersen			
$t_0$	0.0206	0.0207	0.0208
$t_2$	$6.4 \times 10^{-4}$	$6.5 \times 10^{-4}$	$6.7 \times 10^{-4}$
$t_3$	$5.2 \times 10^{-6}$	$3.5 \times 10^{-6}$	$1.6 \times 10^{-6}$
$v_1$	0.0764	0.0760	0.0755
$v_2$	0.0021	0.0020	0.0020
$v_3$	$-1.3 \times 10^{-5}$	$-4.4 \times 10^{-6}$	$+3.5 \times 10^{-6}$
Using phase shifts of Schenk, solution B:			
$t_0$	0.0067	0.0065	0.0063
$t_2$	$4.6 \times 10^{-4}$	$4.8 \times 10^{-4}$	$5.1 \times 10^{-4}$
$t_3$	$1.4 \times 10^{-5}$	$9.9 \times 10^{-6}$	$6.9 \times 10^{-6}$
$v_1$	0.0697	0.0695	0.0693
$v_2$	0.0021	0.0020	0.0020
$v_3$	$-8.4 \times 10^{-7}$	$2.3 \times 10^{-6}$	$6.5 \times 10^{-6}$

<sup>5</sup>For a recent review of experimental  $\pi$ - $\pi$  scattering data, see [25,26].

TABLE II. Comparison of the left- and right-hand sides of Eqs. (3.7a) and (3.7b), using phase shifts of Froggatt and Petersen.

Energy	I=0		I=1		I=2	
	LHS	RHS	LHS	RHS	LHS	RHS
300	0.342	0.344	0.005	0.006	-0.029	-0.029
320	0.377	0.376	0.014	0.012	-0.043	-0.041
340	0.414	0.411	0.022	0.019	-0.055	-0.052
360	0.447	0.445	0.028	0.027	-0.067	-0.064
380	0.479	0.477	0.039	0.037	-0.080	-0.076
400	0.509	0.507	0.049	0.047	-0.090	-0.087
420	0.534	0.534	0.058	0.058	-0.100	-0.099
440	0.557	0.556	0.072	0.071	-0.113	-0.110
460	0.573	0.572	0.088	0.086	-0.122	-0.121
480	0.584	0.585	0.105	0.103	-0.132	-0.132
500	0.590	0.591	0.123	0.122	-0.142	-0.143
520	0.590	0.591	0.146	0.144	-0.152	-0.153
540	0.585	0.586	0.171	0.170	-0.161	-0.163
560	0.574	0.576	0.199	0.199	-0.171	-0.172
580	0.558	0.558	0.234	0.233	-0.178	-0.181
600	0.537	0.538	0.272	0.273	-0.186	-0.189
620	0.512	0.513	0.318	0.319	-0.194	-0.196
640	0.483	0.484	0.371	0.371	-0.201	-0.203
660	0.450	0.450	0.428	0.429	-0.209	-0.209
680	0.414	0.413	0.486	0.490	-0.214	-0.214
700	0.375	0.373	0.532	0.531	-0.222	-0.217

ues of  $\text{Re}f_a^{\text{RHS}}$  and  $\text{Re}f_a^{\text{LHS}}$  are compared in Table II, for 21 energies included in the sum (5.13). We thus conclude that the Froggatt-Petersen phases indeed give a solution of our set of triply subtracted Roy equations, for the values of parameters  $t_i$  and  $v_i$  summarized in Table I. [Notice that the parameters  $t_3$  and  $v_3$  are poorly determined, but that they are sufficiently small not to affect the analysis at the  $O(p^4)$  level.] The corresponding low-energy amplitude  $A_{\text{expt}}(s|tu)$  will be confronted with the theoretical prediction  $A_{\text{th}}$  shortly.

$K_{e4}$ -decay experiments [29] are consistent with the value  $a_0 = 0.30$  for the scattering length, characteristic of Froggatt-Petersen phases, but standard  $\chi$ PT predicts a lower value, namely,  $a_0 = 0.20 \pm 0.01$  [2] (see Fig. 2). It would be desirable to have complete sets of phase shifts that fit both experiment and Roy equations for other values of  $a_0 < 0.30$ . These are not available.<sup>6</sup> For this reason, we must use *ad hoc* extrapolations down to threshold of existing data at energies  $E > 500$ –600 MeV obtained from  $\pi N \rightarrow \pi\pi N$  and  $\pi N \rightarrow \pi\pi\Delta$  production experiments. One such extrapolation has been recently considered by Schenk [30] using a simple parametrization

$$\tan \delta_i(s) = \sqrt{\frac{s-4}{s}} \left[ a_i + \tilde{b}_i \left( \frac{s-4}{4} \right) + c_i \left( \frac{s-4}{4} \right)^2 \right] \left( \frac{4-s_i}{s-s_i} \right) \quad (5.14)$$

$$\tilde{b}_i = b_i - a_i \frac{4}{s_0 - 4} + (a_i)^3.$$

for the two  $s$  waves ( $i = 0, 2$ ) and a similar formula for the  $p$  wave. The scattering lengths  $a_i$  and the slope parameters  $b_i$  are fixed at their values predicted by the standard one-loop  $\chi$ PT [3]:

$$a_0 \equiv a_0^0 = 0.20, \quad a_2 \equiv a_0^2 = -0.042, \quad a_1 \equiv a_1^1 = 0.037 \quad (5.15)$$

$$b_0 \equiv b_0^0 = 0.24, \quad b_2 \equiv b_0^2 = -0.075.$$

The remaining parameters are determined by fitting the data obtained from various analyses of dipion production experiments [28]. For the  $I = 0$   $s$  wave, Schenk uses the

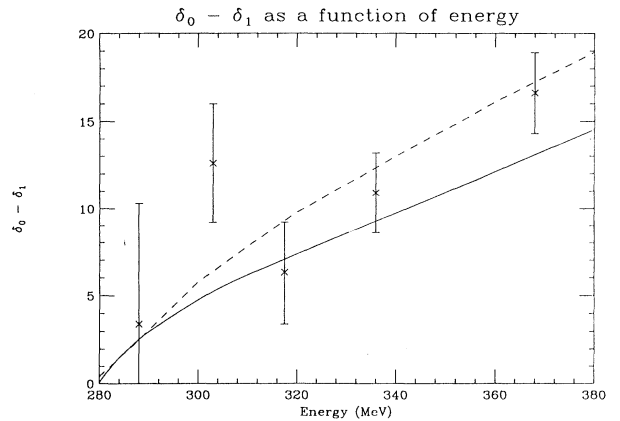


FIG. 2. Phase shift  $\delta_0 - \delta_1$  from data sets of Froggatt and Petersen [17] (dashed curve) and Schenk B [30] (solid curve) compared with experimental data [29] from  $K_{e4}$  decay.

<sup>6</sup>J.L. Basdevant (private communication).

Ochs energy-independent analysis<sup>7</sup> of the CERN-Munich experiment [27], covering the energy range 610–910 MeV. For his best fit, called solution *B*, no  $\chi^2$  or error bars are quoted. Instead, two additional sets of parameters  $c_0$  and  $s_0 = E_0^2$  called *A* and *C* are given that bracket together both the Ochs data and the well-known data by Estabrooks and Martin [27]. A similar procedure is adopted for the  $I = 2$  *s* wave, whereas the parameters of the *p* wave are determined from the experimental  $\rho$  mass and width. Results of this analysis and more details can be found in Ref. [30].

In this way, the parametrization (5.14) provides a complete set of phases, hereafter referred to as Schenk *B*, that fits the data at higher energies and uses the threshold parameters (5.15) of the standard  $\chi$ PT. Using this set, we have performed exactly the same kind of fit to the Roy-type Eqs. (3.7a) and (3.7b) as in the case of Froggatt-Petersen phases. Surprisingly enough, we find this fit at least as good as in the case of the Froggatt-Petersen phases, despite the fact that the Schenk *B* phases were not obtained using Roy equations or any other crossing-symmetry correlation among the three lowest partial waves.<sup>8</sup> The resulting parameters  $t_i$  and  $v_i$  are given in the second half of Table I, and the quality of the fit can be appreciated from Table IV. Unfortunately, we do not see any simple way to associate the Schenk *B* phases, and the corresponding parameters  $t_i$  and  $v_i$ , with a set of errors, which would be deduced from statistical errors of the experimental data used at the beginning and which would respect the correlations imposed by the Roy equations. The same remark applies to the set of phases of Froggatt and Petersen.

### C. Determination of parameters $\alpha$ , $\beta$ , $L_1$ , $L_2$ , and $L_3$ from a complete set of phase shifts

The next step is to confront the empirical amplitude  $A_{\text{expt}}$  with the amplitude  $A_{\text{th}}$  computed from chiral perturbation theory. In particular, the two solutions of the Roy-type equations (3.7a) and (3.7b) described above can be used to measure the parameters  $\alpha, \beta$  and, through Eqs. (4.42), two linear combinations of the low-energy constants  $L_1^2$ ,  $L_2^2$ , and  $L_3$ , defining the four-derivative terms in  $\mathcal{L}_{\text{eff}}$ . The measurement is based on Eqs. (5.10). First, one evaluates the three functions  $\phi_a(s)$ ,  $a = 0, 1, 2$ , defined in Eqs. (5.4), using the complete sets of phase shifts exhibited in Sec. VB. The results are represented graphically by continuous lines in Fig. 3 for the case of Froggatt-Petersen phases and in Fig. 4 for the Schenk *B* set. Next, one fits the experimental functions  $\phi_a(s)$  with

TABLE III. Data from energy-independent analysis of Ochs [31].

Energy (MeV)	$\delta_0$ (deg)
610	$56.3 \pm 3.2$
630	$59.5 \pm 2.9$
650	$65.6 \pm 3.2$
670	$62.5 \pm 3.5$
690	$68.8 \pm 3.6$
710	$74.5 \pm 3.8$
730	$79.4 \pm 3.6$
750	$81.2 \pm 5.7$
770	$79.9 \pm 3.9$
790	$77.5 \pm 5.7$
810	$84.1 \pm 3.3$
830	$84.4 \pm 2.6$
850	$87.1 \pm 2.5$
870	$89.2 \pm 2.5$
890	$93.2 \pm 2.9$
910	$103.3 \pm 3.2$

the theoretical expression represented on the right-hand side of Eqs. (5.10). The parameters of the fit are  $\alpha, \beta$  and  $\tau_0, \tau_1, \tau_2$ . [Recall that the  $\kappa_a$  are defined in terms of the ratio  $\alpha/\beta$ —see Eq. (4.34).]

The range in  $s$  in which the fit is performed should not exceed the range in which the  $O(p^4)$ -order  $\chi$ PT may actually be expected to apply. On the other hand, this range should be large enough to permit a sensitive determination of parameters. For this reason, it might be misleading to consider exclusively the physical region  $s \geq 4$  [4,26]. In the following, we use the interval  $-4 \leq s \leq 8$ , which most likely represents a rather conservative choice.

From Figs. 3 and 4 one observes a large difference in scale of individual  $\phi_a$ :  $\phi_0$  is typically an order of magnitude or more larger than  $\phi_2$  and nearly two orders of magnitude larger than  $\phi_1$ . For this reason, we first fit the function  $\phi_0$ , determining the three parameters  $\alpha, \beta$ , and  $\tau_0$ . Then, using the values of  $\alpha$  and  $\beta$  obtained in this way, we perform two single-parameter fits to  $\phi_2$  and  $\phi_1$ , determining  $\tau_2$  and  $\tau_1$  respectively. In the absence of error bars for  $\phi_a(s)$ , it is impossible to perform a true  $\chi^2$  fit. Instead, we minimize the sum of squares of the difference between the left- and right-hand sides of Eqs. (5.10), for 66 equidistant points in the interval  $-4 \leq s \leq 8$ , giving the same weight to each point.

In all cases, the parameter  $\beta = F_\pi^2/F_0^2$  should remain close to 1, and the fit should be constrained by this condition. We require

$$\beta \leq 1.17, \quad (5.16)$$

corresponding to the lower bound  $F_0 \geq 86$  MeV. This bound is consistent both with existing standard  $\chi$ PT estimates [3] and with the improved  $\chi$ PT formula (4.20). Leaving the ratio  $\alpha/\beta$  unconstrained in the minimization procedure, one tests, for a given set of data, the relevance of the improved  $\chi$ PT. The corresponding fits are represented by dashed curves in Figs. 3 and 4. The corresponding best values of the parameters are

<sup>7</sup>The data by Ochs can be found in his unpublished thesis [31]. We are indebted to Dr. J. Gasser for communicating these unpublished data to us. For the reader's convenience, they are reproduced in our Table III.

<sup>8</sup>A. Schenk (private communication).

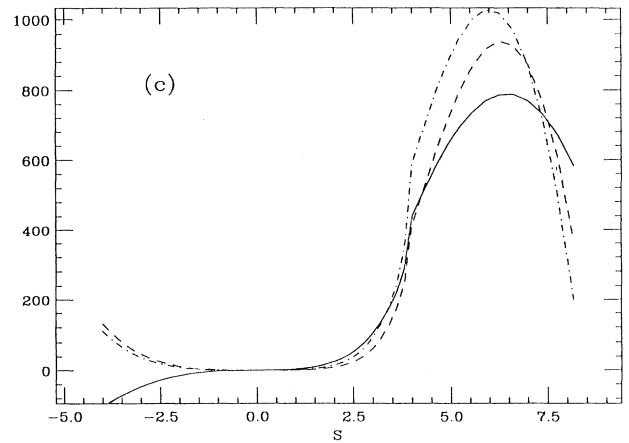
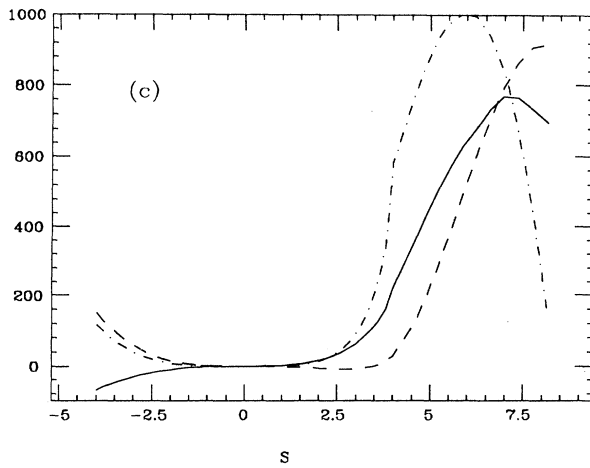
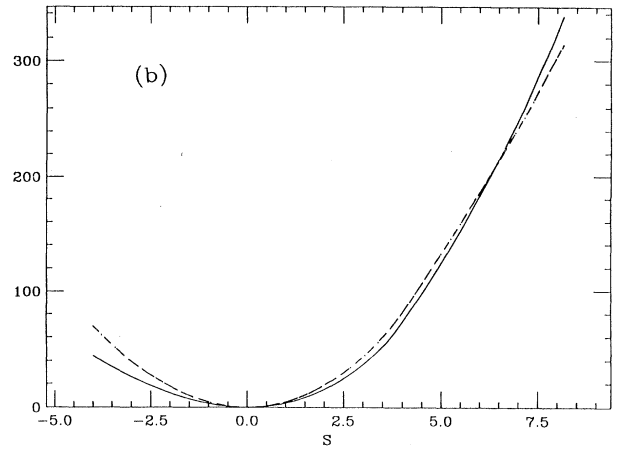
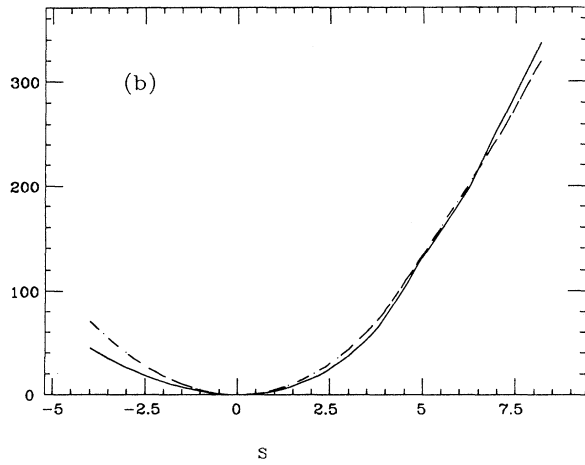
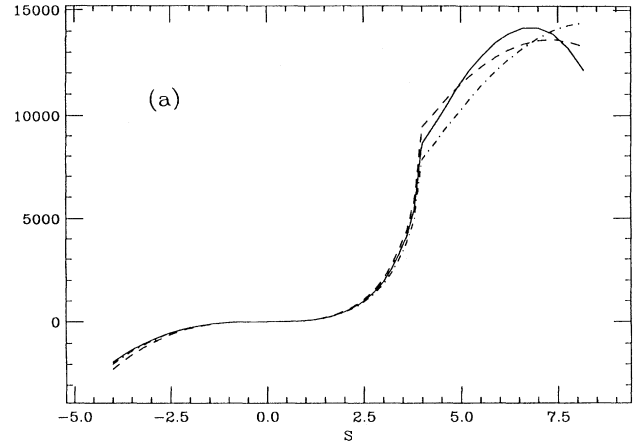
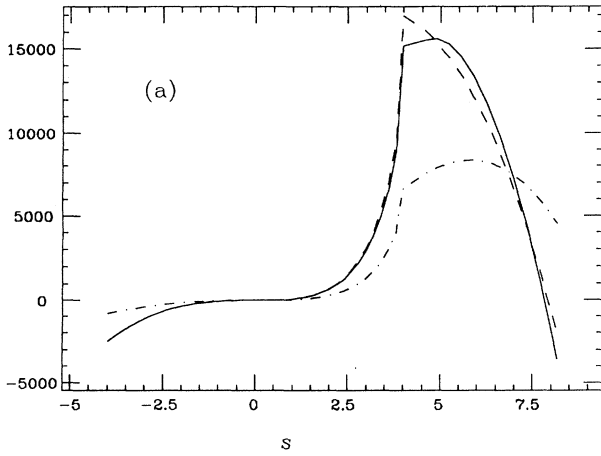


FIG. 3. The functions  $\phi_a$  (shown as solid curves) for (a)  $a = 0$ , (b)  $a = 1$ , and (c)  $a = 2$ , using experimental phase shifts given by Froggatt and Petersen [17]. Comparison is made with theoretical fits: those of the standard  $\chi$ PT are shown as dot-dashed curves, while the improved  $\chi$ PT fits are shown as dashed curves.

FIG. 4. The functions  $\phi_a$  (shown as solid curves), using phase shifts from the Schenk  $B$  [30] parametrization of the phase shifts of Ochs [31]. The meaning of the curves is the same as in Fig. 3.

TABLE IV. Comparison of the left- and right-hand sides of Eqs. (3.7a) and (3.7b), using phase shifts of Schenk, solution  $B$ .

Energy	$I=0$		$I=1$		$I=2$	
	LHS	RHS	LHS	RHS	LHS	RHS
300	0.236	0.234	0.006	0.005	-0.053	-0.052
320	0.274	0.272	0.012	0.011	-0.064	-0.063
340	0.314	0.312	0.019	0.018	-0.075	-0.074
360	0.356	0.355	0.027	0.026	-0.087	-0.085
380	0.398	0.397	0.035	0.034	-0.098	-0.097
400	0.439	0.440	0.045	0.044	-0.109	-0.108
420	0.479	0.479	0.056	0.055	-0.121	-0.119
440	0.515	0.515	0.068	0.067	-0.132	-0.130
460	0.545	0.546	0.083	0.081	-0.143	-0.142
480	0.569	0.569	0.099	0.098	-0.153	-0.153
500	0.584	0.584	0.117	0.116	-0.164	-0.164
520	0.589	0.590	0.138	0.138	-0.174	-0.174
540	0.585	0.585	0.163	0.163	-0.184	-0.185
560	0.571	0.571	0.192	0.192	-0.194	-0.195
580	0.548	0.547	0.226	0.227	-0.203	-0.204
600	0.517	0.517	0.267	0.268	-0.212	-0.213
620	0.480	0.479	0.315	0.316	-0.221	-0.222
640	0.439	0.439	0.370	0.372	-0.229	-0.230
660	0.395	0.394	0.433	0.437	-0.237	-0.237
680	0.350	0.350	0.496	0.495	-0.244	-0.244
700	0.304	0.305	0.540	0.538	-0.252	-0.249

$$\alpha/\beta = 4.20, \quad \beta = 1.17, \quad (5.17a)$$

$$\tau_0 = -0.263, \quad \tau_1 = 3.75, \quad \tau_2 = -0.540,$$

for the set of Froggatt-Petersen phases, and

$$\alpha/\beta = 1.63, \quad \beta = 1.17, \quad (5.17b)$$

$$\tau_0 = -0.032, \quad \tau_1 = 3.68, \quad \tau_2 = -0.640,$$

for phases of the Schenk  $B$  set. On the other hand, in order to test the compatibility of the  $O(p^4)$  standard  $\chi$ PT with a given set of data, one further restricts the fit by requiring

$$\alpha = \beta \leq 1.17. \quad (5.18)$$

Results of the minimization with this constraint are represented by dot-dashed curves in Figs. 3 and 4. The best values of parameters corresponding to this constrained fit are

$$\alpha = \beta = 1.17, \quad \tau_0 = -0.414, \quad \tau_1 = 3.75, \quad \tau_2 = -0.661 \quad (5.19a)$$

and

$$\alpha = \beta = 1.17, \quad \tau_0 = -0.045, \quad \tau_1 = 3.68, \quad \tau_2 = -0.653 \quad (5.19b)$$

for the Froggatt-Petersen and Schenk  $B$  sets of phases, respectively.

A few remarks are in order. The Froggatt-Petersen

data are considerably better fit in terms of a larger value (5.17a) of the ratio  $\alpha/\beta$  than the standard  $\chi$ PT would permit, although without a true  $\chi^2$  fit we cannot be quantitative about this observation. The failure of standard  $\chi$ PT to describe the Froggatt-Petersen  $s$  wave is also apparent in Fig. 3(a) (dot-dashed curve). Concerning the  $p$  wave, the fit is reasonably good for both cases [Fig. 3(b)], reflecting the fact that the theoretical calculation of  $\phi_1(s)$  senses the effective infrared dimension of the quark mass starting only at the two-loop level. It is worth noting that the best value  $\alpha/\beta = 4.20$  is over-critical by 5%. This means that the Froggatt-Petersen  $I=0$   $s$  wave would be compatible with the vanishing of the  $\bar{q}q$  condensate  $B_0$ .<sup>9</sup> From this point of view, the set of Froggatt-Petersen phases with  $a_0^0 = 0.30$  appears as an extreme alternative. The opposite extreme is represented by the Schenk  $B$  set of phases. Since the latter incorporates *a priori* the values of scattering lengths and effective ranges as predicted by the standard  $\chi$ PT, it is not surprising that the corresponding best value for  $\alpha/\beta$  (5.17b) is considerably closer to 1 than in the Froggatt-Petersen case. Furthermore, Fig. 4(a) seems to indicate that, although the best value for  $\alpha/\beta$  is still as large as 1.63, this fact need not be significant. In the absence of error analysis, it is hard to be too affirmative in the interpretation of the Schenk  $B$  fit.

It remains to exploit the additional information (values of constants  $t$  and  $v$  as well as the constants  $\tau$  resulting

<sup>9</sup>This critical case has been considered earlier [32].

from our fits), in order to measure certain parameters of the dimension-4 component of  $\mathcal{L}_{\text{eff}}$ . Here, we merely concentrate on the constants  $L_1$ ,  $L_2$ , and  $L_3$  characteristic of  $\mathcal{L}_{40}$ , Eq. (4.31), whose meaning and renormalization do not depend on the effective dimension of the quark mass. For this purpose, we have to determine the constants  $\alpha_0(0)$  and  $\beta_0(0)$  given by Eqs. (5.11a). Using the central values of the parameters  $t_2$  and  $v_2$  (the second column of Table I) and the best values for  $\alpha/\beta$  and the  $\tau$ 's, as determined in the previous fits, one gets  $\alpha_0(0) = 5.81 \times 10^{-4}$ ,  $\beta_0(0) = 3.99 \times 10^{-3}$  for the Froggatt-Petersen solution, and  $\alpha_0(0) = 5.87 \times 10^{-4}$ ,  $\beta_0(0) = 2.07 \times 10^{-3}$  for the case of Schenk B phases. These numbers are easily converted into information on the constants  $L_{1,2,3}$ , using Eqs. (4.42) and (4.43). Assuming the Zweig-rule (or large- $N_c$ ) relation  $L_2^r - 2L_1^r = 0$ , and identifying the running scale  $\bar{\mu}$  with the  $\eta$  mass, as done in Refs. [3,33], one obtains

$$L_2^r = 2L_1^r = 1.34 \times 10^{-3}, \quad L_3 = -4.50 \times 10^{-3} \quad (5.20a)$$

for the Froggatt-Petersen data, and

$$L_2^r = 2L_1^r = 0.56 \times 10^{-3}, \quad L_3 = -2.15 \times 10^{-3} \quad (5.20b)$$

for the set of Schenk B phases. It is gratifying to see that these values, especially (5.20a), compare well with other determinations based on *standard*  $\chi$ PT [3,33]. Indeed, there is no reason why the purely derivative terms in  $\mathcal{L}_{\text{eff}}$  should be affected by questions concerning the symmetry-breaking sector.

#### D. Estimates of errors in the direct measurements of $\alpha/\beta$

The uncertainties in the values of the parameters  $\alpha$ ,  $\beta$  and  $\tau_a$  arise from uncertainties in the functions  $\phi_a$ ; these uncertainties, in turn, arise from uncertainties in the phase shifts  $\delta_a$  over the range of integration in Eqs. (5.4). As we have noted, there is no set of phase shifts  $\delta_a$  that exists, together with corresponding errors, in this energy range. In the present subsection, we extend the extrapolation method of Schenk [30], described above, to construct several sets of  $I = 0$  phase shifts  $\delta_0$ , together with estimated errors, in the necessary energy interval. In this way, we obtain values and estimated errors for the parameters  $\alpha/\beta$  and  $\tau_0$  for each extrapolated data set. Only  $I = 0$  phases are considered. In fact, we could treat  $I = 1$  phases similarly (although the insensitivity of  $\phi_1$  to  $\alpha$  makes this relatively uninteresting); in any case, the paucity of experimental data on  $I = 2$  makes the production of a complete set of phase shifts impossible without a more extensive recourse to the use of the Roy equations, as in the analysis of Basdevant, Froggatt, and Petersen [23].

The two original sets of phase shifts (with corresponding errors) used are that of Ochs and that of Estabrooks and Martin. These were each obtained independently from analysis of the same CERN-Munich experiment. The first step is to extrapolate  $\delta_0$  down to threshold, using the Schenk formula (5.14). The Ochs phases are fit over the energy range 610–910 MeV, i.e., using all his data for which no inelasticity is suggested. (See Table III.) The Estabrooks-Martin phases are fit over the en-

ergy range 570–910 MeV, i.e., using all their points in the elastic scattering region except for their first three lowest-energy points, which appear to be less trustworthy. In performing the extrapolation, the scattering length  $a_0$  is fixed and the remaining parameters  $b_0, c_0, E_0$  are determined by minimization of  $\chi^2$  using the phases and errors given to us. We show in Fig. 5 the results of this fitting procedure for the choices  $a_0 = 0.20$  (preferred by standard  $\chi$ PT) and 0.26 (preferred by  $K_{e4}$ -decay experiment) for each of the two data sets; the resulting parameters are given in the second through fifth columns of Table V. The  $\chi^2$  for these fits is quite good. (We note in passing that the data of Estabrooks and Martin is not well described by the parameters  $a_0 = 0.20$ ,  $b_0 = 0.24$  which characterize the Schenk B solution.) The next step is to estimate the uncertainty in the extrapolated phases  $\delta_0$ . Since the dominant parameter (after  $a_0$ , which is fixed) is  $b_0$ , and in view of the strong correlations among the parameters, we proceed as follows: For fixed values of  $b_0$  larger than its value for  $\chi^2_{\text{min}}$ , the minimum- $\chi^2$  value, fit the data by allowing  $c_0$  and  $E_0$  to vary freely, and find the values

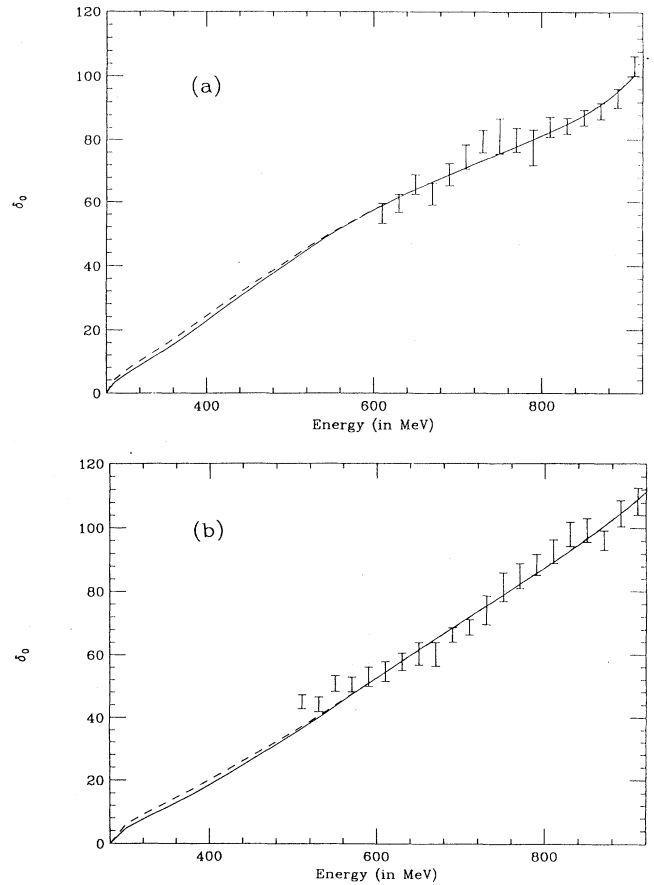


FIG. 5. (a) Schenk-type parametrization of phase shift data of Ochs, fixing  $a_0 = 0.20$  (solid curve) and  $a_0 = 0.26$  (dashed curve); (b) Schenk-type parametrization of phase shift data of Estabrooks and Martin, fixing  $a_0 = 0.20$  (solid curve) and  $a_0 = 0.26$  (dashed curve). Details are given in the text.

TABLE V. Analysis of  $\phi_0$  based on the phase shift data of Ochs and of Estabrooks and Martin (EM), extrapolated to threshold, for fixed values of the scattering length  $a_0$ , using the parametrization of Schenk.

Data	$b_0$	$c_0$	$E_0$	$\chi^2/N_{\text{DF}}$	$\alpha/\beta$	$\tau_0$	$\chi^2/N_{\text{DF}}$ (imprvd.)	$\chi^2/N_{\text{DF}}$ (stand.)
$a_0 = 0.20$								
Ochs "a"	0.393	-0.0356	867.8	11/13				
Ochs "b"	0.348	-0.0292	863.3	10/13	2.32(4)	-0.094(6)	67/63	690/63
Ochs "c"	0.298	-0.0206	858.8	11/13				
EM "a"	0.253	-0.0184	818.6	15/15				
EM "b"	0.229	-0.0147	814.0	14/15	1.581(3)	-0.236(5)	30/63	677/63
EM "c"	0.205	-0.0109	809.6	15/15				
$a_0 = 0.26$								
Ochs "a"	0.369	-0.0339	867.4	11/13				
Ochs "b"	0.324	-0.0274	863.1	10/13	3.50(3)	-0.154(6)	48/63	2328/63
Ochs "c"	0.274	-0.0188	858.6	11/13				
EM "a"	0.227	-0.0163	817.8	14/15				
EM "b"	0.203	-0.0126	813.3	13/15	2.86(3)	-0.305(2)	73/63	4947/63
EM "c"	0.179	-0.0087	808.9	14/15				

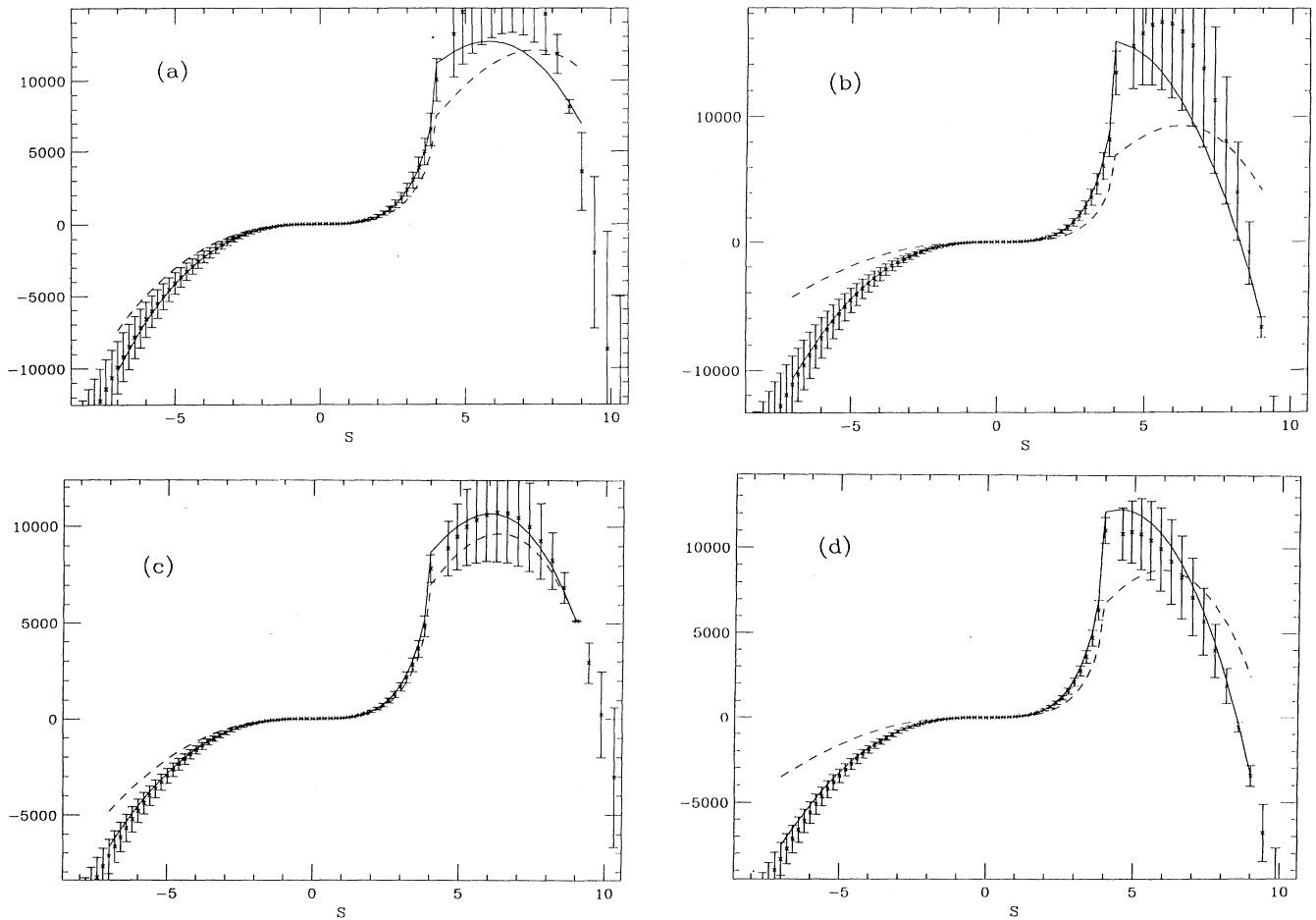


FIG. 6. The function  $\phi_0$  (shown as points with error bars), using Schenk-type parametrization of phase shift data: (a) data of Ochs, fixing  $a_0 = 0.20$ ; (b) data of Ochs, fixing  $a_0 = 0.26$ ; (c) data of Estabrooks and Martin, fixing  $a_0 = 0.20$ ; (d) data of Estabrooks and Martin, fixing  $a_0 = 0.26$ . In each case, the solid curve represents the parametrization of improved  $\chi$ PT, while the dashed curve represents that of standard  $\chi$ PT.

of  $b_0, c_0, E_0$  which give  $\chi^2 = \chi_{\min}^2 + 1$ ; call this solution “ $a$ ” in analogy with Schenk’s notation; repeat this procedure for fixed values of  $b_0$  smaller than that for  $\chi_{\min}^2$ ; call this solution “ $c$ ”; the uncertainty in the phase shift  $\delta_0(E_i)$ , for each value of  $E = E_i$ , is then estimated by interpreting the variation of  $\delta_0(E_i)$  from its solution “ $a$ ” value to its solution “ $c$ ” value as  $\pm 1$  standard deviation in  $\delta_0(E_i)$ . (This is similar to the procedure adopted by Schenk, although he allows much greater variation, leading to much larger uncertainties, in order to bracket both Ochs and Estabrooks-Martin phases at the same time.)

Now, for each of the four sets of phase shifts  $\delta_0$ , obtained by the extrapolation procedure described above, we may make the comparison for  $\phi_0$  as done for the Froggatt-Petersen and Schenk  $B$  phases in Sec. IV C. However, we now have the important advantage that a true  $\chi^2$  fit is possible, so we can have some idea of the precision with which the resulting parameters are determined. For each set, we make two fits: one, corresponding to standard  $\chi$ PT, for which we fix  $\alpha = \beta \leq 1.17$ ; the other, corresponding to improved  $\chi$ PT, for which  $\beta \leq 1.17$  but  $\alpha$  is allowed to vary freely. The fits are all performed over the same interval  $-7 \leq s \leq 9$ . Results of the determination of the parameters  $\alpha/\beta$  and  $\tau_0$  are given in the sixth through ninth columns of Table V; the reader can judge the quality of the fits from the plots of  $\phi_0$  given in Fig. 6. The solid curves represent the parametrization of improved  $\chi$ PT, while the dashed curves represent that of standard  $\chi$ PT. It is clear, both from the large  $\chi^2$  values tabulated for the standard  $\chi$ PT fits and from examination of the dashed curves in Fig. 6 that standard  $\chi$ PT is not compatible with these phase shifts. For this reason, we quote no result for  $\tau_0$  for this case. On the other hand, improved  $\chi$ PT can easily accommodate such data. It is important to note that, for a given set of phase shifts, the parameters  $\alpha/\beta$  and  $\tau_0$  are very well determined by the improved  $\chi$ PT fit.

As a check on our procedure of estimating errors, we have also used a more “conservative” procedure, viz., vary all nonfixed parameters within their one-standard-deviation limits to produce solution “ $a_{\text{cons}}$ ,” taking  $\max(b_0), \max(c_0), \min(s_0)$ , and solution “ $c_{\text{cons}}$ ,” taking  $\min(b_0), \min(c_0), \max(s_0)$ ; then compute the conservative uncertainties in the phase shifts  $\delta_0(E_i)$  using these solutions as we did for solutions  $a$  and  $c$  before. Clearly, this method does not take into account the strong correlations in  $b_0, c_0, s_0$ . Thus, when the consequent phase-shift errors are used in the fitting of  $\phi_0$ , these larger errors result in larger errors in the experimental function  $\phi_0$ . The result is then a  $\chi^2$  roughly half of that previously obtained, and errors in  $\alpha/\beta$  and  $\tau_0$  roughly 2–5 times larger. Nevertheless, the best fit is the same.

## VI. SUMMARY AND CONCLUSIONS

A new framework for testing the convergence rate of chiral perturbation theory is proposed. One first replaces the standard expansion of the effective Lagrangian by a more general expansion that is as systematic and unambiguous as the standard  $\chi$ PT. In addition to the usual

terms, the new expansion involves at each given order new contributions that the standard  $\chi$ PT relegates to higher orders. The size of these additional contributions can then be tested experimentally, in particular in low-energy  $\pi$ - $\pi$  scattering. Unless these contributions turn out to be small, the improved  $\chi$ PT has, in principle, more chance to produce a rapidly convergent expansion scheme.

A new low-energy theorem is presented, which provides the general solution of constraints imposed by analyticity, crossing symmetry and unitarity on the  $\pi$ - $\pi$  scattering amplitude, neglecting  $O(p^8)$  contributions. Applications of this theorem are threefold.

(i) First, it considerably simplifies the evaluation of the perturbative  $\pi$ - $\pi$  amplitude up to and including two loops. This applies both within the “standard  $\chi$ PT” and within the more general “improved  $\chi$ PT,” which contains the former as a special case. In both cases, the calculation reduces to the iterative insertion of the unitarity condition (4.32) into the dispersive integral for the functions  $T$ ,  $U$ , and  $V$  in Eq. (3.2). The improved  $\chi$ PT one-loop amplitude is worked out in detail in Sec. IV. The two-loop amplitude can be easily calculated along the same lines. The reason why the formula (3.2) no longer holds beyond two loops resides in new  $O(p^8)$  effects in the absorptive part: inelasticities and higher partial waves.

(ii) Next, the low-energy theorem of Sec. III can be used to constrain the low-energy scattering data and to fully reconstruct the corresponding amplitude. The formula (3.2) implies a particular truncation of the infinite system of Roy equations, under a rigorous control of chiral power counting: Neglected contributions are  $O(p^8)$ , whereas in the original form of the Roy equations [20] the model-dependent “driving terms” are of the same order  $O(p^4)$  as the effects we are looking for. A complete set of low-energy phases  $\delta_0^0, \delta_0^2$ , and  $\delta_1^1$ , together with the six subtraction constants  $t$  and  $v$  for which the Roy-type Eqs. (2.7a) and (2.7b) are satisfied to a reasonable accuracy (see Tables II and IV), define up to  $O(p^8)$  corrections the scattering amplitude  $A(s, t, u)$  in a whole low-energy region of the Mandelstam plane including the unphysical region. Two examples of such a complete low-energy amplitude are given, based on phase shifts published by Froggatt and Petersen [17] and by Schenk [30], respectively. They are both compatible with existing  $\pi N \rightarrow \pi\pi N$  and  $K_{e4}$  experimental data.

(iii) Finally, the low-energy representation (3.2) simplifies the direct comparison of the perturbative amplitude  $A^{\text{th}}(s, t, u)$  with the amplitude  $A^{\text{expt}}(s, t, u)$  reconstructed from the data. In particular, parameters of  $\mathcal{L}_{\text{eff}}$  contained in  $A^{\text{th}}$  can be measured through a detailed fit of the amplitude  $A^{\text{expt}}(s, t, u)$  over a sufficiently large portion of the Mandelstam plane in which the low-energy expansion can still be taken as valid. The fit is particularly sensitive to the ratio  $\alpha/\beta$ , which parametrizes the leading  $O(p^2)$  amplitude. The improved  $\chi$ PT requires  $1 \leq \alpha/\beta \leq 4$ , whereas the special case of the standard  $\chi$ PT corresponds to  $\alpha/\beta = 1$ . The ratio  $\alpha/\beta$  is related to the value of the QCD parameter  $2\hat{m}B_0$  in the units of pion mass squared and, *via* the pseudoscalar mass spectrum, to the quark mass ratio  $r = m_s/\hat{m}$ .

Examples of measurement of  $\alpha/\beta$  exhibited in this paper illustrate the lack of sufficiently precise experimental information on low-energy  $\pi$ - $\pi$  scattering. For a fixed value of the scattering length  $a_0^0$ , the statistical errors of the production data on  $\delta_0^0$  are estimated to show up as errors in the measured values of  $\alpha/\beta$  of the order of a few percent. On the other hand, for different values of  $a_0^0$  in the experimental range  $a_0^0 = 0.26 \pm 0.05$ , and for different sets of production data, the resulting values of  $\alpha/\beta$  vary between 1.5 and 4.2. The two complete low-energy amplitudes mentioned above correspond to these two extremes. In particular, the Froggatt-Petersen phases (for which  $a_0^0 = 0.30$ ) are compatible with the vanishing of the condensate  $B_0$  and with the critical value of the quark mass ratio  $r = r_1 \simeq 6.3$ .

The suspicion that a bad convergence of the standard  $\chi$ PT might bias the usual conclusions that  $r = m_s/\hat{m} \simeq 25.9$  and  $2\hat{m}B_0 \simeq M_\pi^2$  is at least well motivated, but clearly it requires confirmation. In order to produce a truly unbiased measurement of these fundamental QCD parameters, the method developed in this paper can prove useful provided that it is supplied with more accurate experimental information on low-energy  $\pi$ - $\pi$  phase shifts. The current imprecision, illustrated by error bars as large as in  $a_0^0 = 0.26 \pm 0.05$  can hide *all* cases of interest, including the intriguing critical case  $\langle \bar{q}q \rangle = 0$ . Here, one faces a challenge of fundamental high-precision low-energy experimental physics.

### ACKNOWLEDGMENTS

We are indebted to Dr. M. Knecht for various discussions and for pointing out some errors in a preliminary version. Discussions on  $\pi$ - $\pi$  data with Dr. J.-L. Basdevant and with Dr. J. Gasser at various stages of this work have been extremely useful. One of us (N.H.F.) would like to thank the Division de Physique Théorique, Orsay, for its generous hospitality and support during his sabbatical leave of absence, and the Department of Physics of Arizona State University for its hospitality as well. The Division de Physique Théorique is a Unité de Recherche of the Universités Paris 11 and Paris 6 associated with CNRS.

### APPENDIX A: NOTATION AND CONVENTIONS

In the first part of this appendix, we fix the notation and normalization for the scattering amplitude. We then

exhibit the main properties of the crossing matrices  $C$  [Eq. (3.9)].

The  $S$ -matrix element for the transition  $\pi^a + \pi^b \rightarrow \pi^c + \pi^d$ , where  $a, b, c, d$  are pion isospin indices, is connected to the  $T$ -matrix element by the relation

$$\langle cd|S|ab \rangle = \langle cd|ab \rangle + i(2\pi)^4 \delta^4(p_a + p_b - p_c - p_d) T_{ab,cd} \quad (\text{A1})$$

The  $T$ -matrix element can be written in terms of isospin invariant amplitudes; taking crossing symmetry into account, the decomposition reads

$$T_{ab,cd}(s, t, u) = A(s|tu)\delta_{ab}\delta_{cd} + A(t|su)\delta_{ac}\delta_{bd} + A(u|ts)\delta_{ad}\delta_{bc}, \quad (\text{A2})$$

where  $s, t$ , and  $u$  are the Mandelstam variables:

$$s = (p_a + p_b)^2, \quad t = (p_a - p_c)^2, \quad u = (p_a - p_d)^2. \quad (\text{A3})$$

The amplitude  $A(s|tu)$  is symmetric in the variables  $t, u$ . [The amplitude  $A(t|su)$  is obtained from  $A(s|tu)$  by the exchange of variables  $s, t$  and by subsequent analytic continuation.]

The  $s$ -channel isospin amplitudes  $F^{(I)}$  [Eq. (3.8)] are related to the amplitude  $A$  by

$$\begin{pmatrix} F^{(0)} \\ F^{(1)} \\ F^{(2)} \end{pmatrix}(s, t, u) = \frac{1}{32\pi} \begin{pmatrix} 3 & 1 & 1 \\ 0 & 1 & -1 \\ 0 & 1 & 1 \end{pmatrix} \begin{pmatrix} A(s|tu) \\ A(t|su) \\ A(u|ts) \end{pmatrix}. \quad (\text{A4})$$

The partial wave expansion is

$$F^{(I)} = \sum_{\ell} (2\ell + 1) P_{\ell}(\cos \theta) f_{\ell}^I(s), \quad (\text{A5})$$

where  $s = 4(M_\pi^2 + q^2)$ ,  $t = -2q^2(1 - \cos \theta)$ . With this normalization, the elastic unitarity condition for  $f_{\ell}^I$  takes the form

$$\text{Im} f_{\ell}^I(s) = \sqrt{\frac{s - 4M_\pi^2}{s}} |f_{\ell}^I(s)|^2, \quad (\text{A6a})$$

$$f_{\ell}^I(s) = \sqrt{\frac{s}{s - 4M_\pi^2}} e^{i\delta_{\ell}^I(s)} \sin \delta_{\ell}^I(s). \quad (\text{A6b})$$

The crossing matrices  $C$  [Eq. (3.9)] have the forms

$$C_{st} = \begin{pmatrix} 1/3 & 1 & 5/3 \\ 1/3 & 1/2 & -5/6 \\ 1/3 & -1/2 & 1/6 \end{pmatrix}, \quad C_{tu} = \begin{pmatrix} 1 & 0 & 0 \\ 0 & -1 & 0 \\ 0 & 0 & 1 \end{pmatrix}, \quad C_{su} = \begin{pmatrix} 1/3 & -1 & 5/3 \\ -1/3 & 1/2 & 5/6 \\ 1/3 & 1/2 & 1/6 \end{pmatrix}, \quad (\text{A7})$$

and satisfy the relations

$$C_{tu}^2 = C_{su}^2 = C_{st}^2 = 1, \tag{A8}$$

$$C_{st}C_{su} = C_{tu}C_{st} = C_{su}C_{tu}, \tag{A9}$$

$$C_{su}C_{st} = C_{tu}C_{su} = C_{st}C_{tu}.$$

It is worthwhile to notice that Eqs. (A9) imply that the eigenvectors  $A_{\pm}$  with eigenvalues  $\pm 1$ , respectively, of the matrix  $C_{tu}$  satisfy

$$C_{su}C_{st}A_{\pm} = \pm C_{st}A_{\pm}. \tag{A10}$$

These relations are extensively used throughout the calculation of Sec. III C.

The invariance of the amplitude  $A(stu)$  under the exchange of the variables  $t, u$  permits us to construct rather easily all independent crossing symmetric polynomials of a given degree in  $s, t, u$ . It is convenient to take the variables  $t, u$  as independent. Since there are

$$k_n \equiv [n/2] + 1 \tag{A11}$$

symmetric monomials in  $t, u$  that are homogeneous of degree  $n$ , the number of independent parameters in a general crossing symmetric polynomial of degree  $N$  is

$$K_N \equiv \sum_{n=0}^N k_n. \tag{A12}$$

Hence, the most general polynomial of degree three contains six parameters, as claimed in Sec. III C.

### APPENDIX B: AMBIGUITIES OF THE AMPLITUDES $T, U, \text{ AND } V$

In this appendix, we determine the general expression for the transformations  $T \rightarrow T + \delta T, U \rightarrow U + \delta U,$  and  $V \rightarrow V + \delta V$  that leave invariant the scattering amplitude  $A$  [Eq. (3.2)]. It follows that the variations  $\delta T, \delta U,$  and  $\delta V$  must satisfy the equation

$$\delta T(s) + \delta T(t) + \delta T(u) + \frac{1}{3}[2\delta U(s) - \delta U(t) - \delta U(u)] + \frac{1}{3}[(s-t)\delta V(u) + (s-u)\delta V(t)] = 0. \tag{B1}$$

In order to solve Eq. (B1), one notices that only two out of the three variables  $s, t, u$  are independent. By successive differentiation with respect to independent variables, one obtains a set of simpler equations, which can be solved easily. To simplify notation, let us define

$$f \equiv \delta T, \quad g \equiv \delta U, \quad h \equiv \delta V. \tag{B2}$$

We first consider  $s$  and  $t$  as independent variables, and differentiate Eq. (B1) first with respect to  $s$  and then with respect to  $t$ . We thus obtain the following two equations, where the primes indicate differentiation with respect to the arguments of the functions:

$$f'(s) - f'(u) + \frac{1}{3}[2g'(s) + g'(u)] + \frac{1}{3}[h(u) + 2h(t)] - \frac{1}{3}(s-t)h'(u) = 0, \tag{B3}$$

$$f''(u) - \frac{1}{3}g''(u) + \frac{2}{3}h'(t) + \frac{1}{3}(s-t)h''(u) = 0. \tag{B4}$$

We now consider  $t$  and  $u$  as independent variables and differentiate Eq. (B4) with respect to  $t$ , obtaining the result

$$h''(t) - h''(u) = 0, \tag{B5}$$

which indicates that  $h''$  is a constant, and therefore  $h$  is

a quadratic polynomial:

$$h(t) = \frac{1}{2}at^2 + bt + c, \tag{B6}$$

where  $a, b, c$  are constants. Using this result for  $h$  in Eq. (B4), we find a relation between  $f$  and  $g$ :

$$f(u) = \frac{1}{3}g(u) + \frac{1}{18}au^3 - \frac{1}{3}(b + 2M_{\pi}^2a)u^2 + du + e, \tag{B7}$$

where  $d$  and  $e$  are constants. We then return to Eq. (B3), consider  $s$  and  $u$  as independent variables, and differentiate with respect to  $s$ . This implies

$$f''(s) + \frac{2}{3}g''(s) - \frac{4}{3}b - \frac{2}{3}a(4M_{\pi}^2 - s) = 0, \tag{B8}$$

which becomes, after replacing  $f$  in terms of  $g$  [Eq. (B7)],

$$g''(s) + as - 2(b + 2M_{\pi}^2a) = 0, \tag{B9}$$

the solution of which is

$$g(s) = -\frac{a}{6}s^3 + (b + 2M_{\pi}^2a)s^2 + ks + \ell, \tag{B10}$$

where  $k$  and  $\ell$  are constants. The expression for  $f$  then becomes

$$f(s) = \left(d + \frac{k}{3}\right)s + \left(e + \frac{\ell}{3}\right). \tag{B11}$$

Finally, upon substituting the expressions for  $h$  [Eq. (B6)],  $g$  [Eq. (B10)], and  $f$  [Eq. (B11)] in the original equation (B1), we obtain two constraints on the constants

$$\left(e + \frac{\ell}{3}\right) = -\frac{4M_\pi^2}{3} \left(d + \frac{k}{3}\right), \quad (\text{B12})$$

$$c = -\left(k + 4M_\pi^2 b + \frac{16}{3}M_\pi^4 a\right). \quad (\text{B13})$$

After relabeling the constants as

$$\begin{aligned} y_0 &= \ell, \quad y_1 = k, \quad y_2 = (b + 2M_\pi^2 a), \\ y_3 &= -a/6, \quad x = d + k/3, \end{aligned} \quad (\text{B14})$$

the functions  $f$ ,  $g$ , and  $h$ , and hence  $\delta T$ ,  $\delta U$ , and  $\delta V$  [Eqs. (B2)] take the forms given in Eqs. (3.5).

### APPENDIX C: POLYNOMIALS AND KERNELS OF THE ROY-TYPE EQUATIONS

In this Appendix we explicitly list the polynomials  $P_a(s)$  and the kernels  $W_{ab}$  which appear in the Roy-type dispersion relations (3.7):

$$\begin{aligned} P_0(s) &= 5t_0 + \frac{5}{9}t_2[3s^2 + 2(s - 4M_\pi^2)^2] + \frac{5}{6}t_3[2s^3 - (s - 4M_\pi^2)^3] \\ &\quad + \frac{2}{9}v_1(3s - 4M_\pi^2) - \frac{8}{27}v_2(s - M_\pi^2)(s - 4M_\pi^2) + \frac{1}{27}v_3(5s - 4M_\pi^2)(s - 4M_\pi^2)^2, \end{aligned} \quad (\text{C1})$$

$$\begin{aligned} P_2(s) &= 2t_0 + \frac{2}{9}t_2[3s^2 + 2(s - 4M_\pi^2)^2] + \frac{1}{3}t_3[2s^3 - (s - 4M_\pi^2)^3] \\ &\quad - \frac{1}{9}v_1(3s - 4M_\pi^2) + \frac{4}{27}v_2(s - M_\pi^2)(s - 4M_\pi^2) - \frac{1}{54}v_3(5s - 4M_\pi^2)(s - 4M_\pi^2)^2, \end{aligned} \quad (\text{C2})$$

$$P_1(s) = \frac{1}{9}(s - 4M_\pi^2)(v_1 + v_2 s) + \frac{2}{27}(s - 4M_\pi^2)v_3[s^2 - \frac{1}{20}(s - 4M_\pi^2)(11s - 4M_\pi^2)], \quad (\text{C3})$$

$$\begin{aligned} \frac{1}{\pi} \int_{4M_\pi^2}^{\Lambda^2} \frac{dx}{x} \sum_{b=0}^2 W_{0b}(s, x) \text{Im } f_b(x) &= \frac{4}{\pi}(s - 4M_\pi^2)^2(s - 2M_\pi^2) \int_{4M_\pi^2}^{\Lambda^2} \frac{dx}{x^3} \frac{\text{Im } f_1(x)}{x - 4M_\pi^2} \\ &\quad - \frac{1}{6\pi}(s - 4M_\pi^2)^3 \int_{4M_\pi^2}^{\Lambda^2} \frac{dx}{x^4} \{ \text{Im } f_0(x) + 5 \text{Im } f_2(x) \\ &\quad + 9 \left(1 + \frac{2s}{x - 4M_\pi^2}\right) \text{Im } f_1(x) \} G\left(\frac{s - 4M_\pi^2}{x}\right), \end{aligned} \quad (\text{C4})$$

$$\begin{aligned} \frac{1}{\pi} \int_{4M_\pi^2}^{\Lambda^2} \frac{dx}{x} \sum_{b=0}^2 W_{2b}(s, x) \text{Im } f_b(x) &= -\frac{2}{\pi}(s - 4M_\pi^2)^2(s - 2M_\pi^2) \int_{4M_\pi^2}^{\Lambda^2} \frac{dx}{x^3} \frac{\text{Im } f_1(x)}{x - 4M_\pi^2} \\ &\quad - \frac{1}{12\pi}(s - 4M_\pi^2)^3 \int_{4M_\pi^2}^{\Lambda^2} \frac{dx}{x^4} \{ 2 \text{Im } f_0(x) + \text{Im } f_2(x) \\ &\quad - 9 \left(1 + \frac{2s}{x - 4M_\pi^2}\right) \text{Im } f_1(x) \} G\left(\frac{s - 4M_\pi^2}{x}\right), \end{aligned} \quad (\text{C5})$$

$$\begin{aligned} \frac{1}{\pi} \int_{4M_\pi^2}^{\Lambda^2} \frac{dx}{x} \sum_{b=0}^2 W_{1b}(s, x) \text{Im } f_b(x) &= -\frac{1}{\pi}(s - 4M_\pi^2)^2(s - 2M_\pi^2) \int_{4M_\pi^2}^{\Lambda^2} \frac{dx}{x^3} \frac{\text{Im } f_1(x)}{x - 4M_\pi^2} \\ &\quad + \frac{1}{12\pi}(s - 4M_\pi^2)^2 \int_{4M_\pi^2}^{\Lambda^2} \frac{dx}{x^3} \left[ 2 - \left(2 + \frac{s - 4M_\pi^2}{x}\right) G\left(\frac{s - 4M_\pi^2}{x}\right) \right] \\ &\quad \times \left\{ 2 \text{Im } f_0(x) - 5 \text{Im } f_2(x) + 9 \left(1 + \frac{2s}{x - 4M_\pi^2}\right) \text{Im } f_1(x) \right\} \end{aligned} \quad (\text{C6})$$

In Eqs. (C4)–(C6), the function  $G$  is defined as

$$G(x) \equiv 4 \int_0^1 dy \frac{y^3}{1 + xy} = \frac{4}{3x} - \frac{2}{x^2} + \frac{4}{x^3} - \frac{4}{x^4} \ln(1 + x), \quad G(0) = 1. \quad (\text{C7})$$

- [1] S. Weinberg, *Physica A* **96**, 327 (1979).
- [2] J. Gasser and H. Leutwyler, *Ann. Phys. (N.Y.)* **158**, 142 (1984).
- [3] J. Gasser and H. Leutwyler, *Nucl. Phys.* **B250**, 465 (1985).
- [4] J. Donoghue, C. Ramirez, and G. Valencia, *Phys. Rev. D* **38**, 2195 (1988).
- [5] M. Gell-Mann, R.J. Oakes, and B. Renner, *Phys. Rev.* **175**, 2195 (1968); S. Glashow and S. Weinberg, *Phys. Rev. Lett.* **20**, 224 (1968).
- [6] N. H. Fuchs, H. Sazdjian, and J. Stern, *Phys. Lett. B* **269**, 183 (1991).
- [7] S. Weinberg, *Phys. Rev. Lett.* **18**, 188 (1967); T. Das, V. Mathur, and S. Okubo, *ibid.* **18**, 781 (1967); G. Ecker, J. Gasser, H. Leutwyler, A. Pich, and E. De Rafael, *Phys. Lett. B* **223**, 425 (1989); G. Ecker, J. Gasser, A. Pich, and E. De Rafael, *Nucl. Phys.* **B321**, 311 (1989); H. Leutwyler, *ibid.* **B337**, 108 (1990); J. F. Donoghue and B. R. Holstein, *Phys. Rev. D* **46**, 4076 (1992).
- [8] Y. Nambu and G. Jona-Lasinio, *Phys. Rev.* **122**, 345 (1961); **124**, 246 (1961).
- [9] S. Weinberg, in *A Festschrift for I.I. Rabi*, edited by L. Motz (New York Academy of Sciences, New York, 1977), p. 185; J. Gasser and H. Leutwyler, *Phys. Rep.* **87**, 77 (1982).
- [10] N. H. Fuchs, H. Sazdjian, and J. Stern, *Phys. Lett. B* **238**, 380 (1990).
- [11] R. Koch and E. Pietarinen, *Nucl. Phys.* **A336**, 331 (1980); see also R. Koch and M. Hutt, *Z. Phys. C* **19**, 119 (1983).
- [12] R.A. Arndt *et al.*, *Phys. Rev. Lett.* **65**, 157 (1990).
- [13] J. Bijnens and F. Cornet, *Nucl. Phys.* **B296**, 557 (1988); J. F. Donoghue, B. R. Holstein, and Y. C. Lin, *Phys. Rev. D* **37**, 2423 (1988); H. Marsiske *et al.*, *ibid.* **41**, 3324 (1990); D. Morgan and M. R. Pennington, *Phys. Lett. B* **272**, 134 (1992); M. R. Pennington, in *The DAΦNE Physics Handbook*, edited by Luciano Maiani, Giulia Pancieri, and Nello Paver (Laboratori Nazionali di Frascati, Frascati, 1991), p. 379.
- [14] J. Gasser and H. Leutwyler, *Nucl. Phys.* **B250**, 539 (1985).
- [15] S. Weinberg, *Phys. Rev. Lett.* **17**, 616 (1966).
- [16] J. L. Petersen, CERN Report No. 77-04, 1975-1976 (unpublished).
- [17] C. D. Froggatt and J. L. Petersen, *Nucl. Phys.* **B129**, 89 (1977).
- [18] M. M. Nagels *et al.*, *Nucl. Phys.* **B147**, 189 (1979); O. Dumbrajs *et al.*, *ibid.* **B216**, 277 (1983).
- [19] J. Donoghue, *Annu. Rev. Nucl. Part. Phys.* **39**, 1 (1989).
- [20] S. M. Roy, *Phys. Lett.* **36B**, 353 (1971); *Helv. Phys. Acta* **63**, 627 (1990); J. L. Basdevant, J. C. Le Guillou, and H. Navelet, *Nuovo Cimento* **7A**, 363 (1972).
- [21] A. S. Eddington, *Proc. R. Soc. London* **A122**, 353 (1929).
- [22] G. F. Chew and S. Mandelstam, *Phys. Rev.* **119**, 467 (1960).
- [23] J. L. Basdevant, C. D. Froggatt, and J. L. Petersen, *Phys. Lett.* **41B**, 173 (1972); **41B**, 178 (1972); *Nucl. Phys.* **B72**, 413 (1974); M. R. Pennington and S. D. Protopopescu, *Phys. Rev. D* **7**, 1429 (1973); **7**, 2591 (1973).
- [24] D. Atkinson and T. P. Pool, *Nucl. Phys.* **B81**, 502 (1974); T. P. Pool, *Nuovo Cimento* **45A**, 207 (1978); A. C. Heemskerck and T. P. Pool, *ibid.* **49A**, 393 (1979).
- [25] W. Ochs,  *$\pi$ -N Newsletter* **3**, 25 (1991).
- [26] J. Gasser and U.-G. Meissner, *Phys. Lett. B* **258**, 219 (1991).
- [27] P. Estabrooks and A. D. Martin, *Nucl. Phys.* **B79**, 301 (1974).
- [28] B. Hyams *et al.*, *Nucl. Phys.* **B64**, 134 (1973); W. Hoogland *et al.*, *ibid.* **B69**, 266 (1974).
- [29] L. Rosselet *et al.*, *Phys. Rev. D* **15**, 574 (1977).
- [30] A. Schenk, *Nucl. Phys.* **B363**, 97 (1991).
- [31] W. Ochs, thesis, Ludwig-Maximilians-Universität, 1973.
- [32] N. H. Fuchs, *Nuovo Cimento Lett.* **27**, 21 (1980); J. Stern, in *Black Forest Meeting on Quark Masses and Lattice Gauge Theories*, Todtnauberg, 1982 (unpublished); J.R. Crewther, *Phys. Lett. B* **176**, 172 (1984); G.A. Christos, *Aust. J. Phys.* **39**, 347 (1986).
- [33] C. Riggenbach, J. Gasser, J. F. Donoghue, and B. R. Holstein, *Phys. Rev. D* **43**, 127 (1991).